Chemistry of Polynuclear Metal Complexes with Bridging Carbene or Carbyne Ligands. Part 66.* Carbaboranetungsten–Platinum Complexes. Polyhedral Rearrangements of a 12-Vertex Cage System; Crystal Structures of $[PtW(CO)_2(PEt_3)_2\{\eta^6\text{-}C_2B_9H_8(CH_2C_6H_4Me\text{-}4)Me_2\}]\cdot CH_2Cl_2$, $[PtW(\mu\text{-}H)\{\mu\text{-}\sigma\text{:}\ \eta^5\text{-}C_2B_9H_7(CH_2C_6H_4\text{-}Me\text{-}4)Me_2\}(CO)_2(PMe_3)(PEt_3)_2]$, and Related Compounds†

Michael J. Attfield, Judith A. K. Howard, Alasdair N. de M. Jelfs, Christine M. Nunn, and F. Gordon A. Stone
Department of Inorganic Chemistry, The University, Bristol BS8 1TS

In acetone, the salts $[N(PPh_3)_2][W(\equiv CC_6H_4Me\text{-}4)(CO)_2(\eta^5\text{-}C_2B_9H_9Me_2)]$ and $[PtH(Me_2CO)(PEt_3)_2][BF_4]$ yield the dimetal compound $[PtW(CO)_2(PEt_3)_2\{\eta^6\text{-}C_2B_9H_8(CH_2C_6H_4Me\text{-}4)Me_2\}]$ (**2a**), the structure of which has been established by *X*-ray diffraction. The very short Pt–W bond [2.602(1) Å] is semi-bridged by the two carbonyl ligands [W–C–O 165(1) and 168(1)°], while a novel $\eta^6\text{-}C_2B_9H_8(CH_2C_6H_4Me\text{-}4)Me_2$ group ligates the tungsten atom. Six atoms BCBBBC in the face of the ligand are within bonding distance of the metal, but the C ••• C separation (2.88 Å) within the ring is non-bonding. The $CH_2C_6H_4Me$-4 substituent is attached to the central boron of the B_3 unit, and is derived from the Pt–H, B–H, and CC_6H_4Me-4 groups present in the reactants. Treatment of $[N(PPh_3)_2][W(\equiv CMe)(CO)_2(\eta^5\text{-}C_2B_9H_9Me_2)]$ with $[PtH(Me_2CO)(PEt_3)_2][BF_4]$ affords an inseparable 1 : 2 mixture of the two complexes $[PtW(CO)_2(PEt_3)_2\{\eta^6\text{-}C_2B_9H_8(R)Me_2\}]$ [(**2b**), R = H; (**2c**), R = Et]. Reactions between (**2a**) and the electron pair donor molecules L = PMe_3, CO, $CNBu^t$, or $PHPh_2$ yield the complexes $[PtW(\mu\text{-}H)\{\mu\text{-}\sigma\text{:}\ \eta^5\text{-}C_2B_9H_7(CH_2C_6H_4Me\text{-}4)Me_2\}(CO)_2(L)(PEt_3)_2]$ (**3**). The structure of (**3a**) (L = PMe_3) was established by *X*-ray diffraction, confirming that the Pt–W bond [2.843(2) Å] is bridged by a hydrido ligand, the presence of which was revealed in the ^1H n.m.r. spectrum. The tungsten atom is ligated by two terminal CO groups, the PMe_3 group, and an $\eta^5\text{-}C_2B_9H_7(CH_2C_6H_4Me\text{-}4)Me_2$ group. In the latter the central boron of the *nido*-C_2B_3 face carries the $CH_2C_6H_4Me$-4 substituent, while another boron atom in the face forms an *exo*-polyhedral bond to the platinum [2.123(5) Å]. The synthesis of (**3a**) from (**2a**) thus represents an unprecedented *iso-closo* (or *hyper-closo*) to *closo* transformation in a C_2B_9W 12-vertex framework. The mixture of compounds (**2b**) and (**2c**) (*ca.* 1 : 2) reacts with CO to give three complexes $[PtW(\mu\text{-}H)\{\mu\text{-}\sigma\text{:}\ \eta^5\text{-}C_2B_9H_7(R)Me_2\}(CO)_3(PEt_3)_2]$ [(**3e**), R = H; (**3f**), R = Et] and $[PtW(CO)_3(PEt_3)_2(\eta^5\text{-}C_2B_9H_9Me_2)]$ (**4**), formed in a ratio (**3e**) : (**3f**) : (**4**) of *ca.* 1 : 4 : 1. Moreover, i.r. and n.m.r. studies showed that there was an equilibrium in solution between (**3e**) and (**4**). Column chromatography on alumina failed to separate the three complexes completely, and an *X*-ray study on a crystal from the mixture revealed that co-crystallisation had occurred. The asymmetric unit contains two crystallographically independent and chemically inequivalent molecules. One molecule proved to be (**4**), having a structure in which the Pt–W bond [2.818(1) Å] is bridged by a B–H → Pt three-centre two-electron linkage. The latter involves the central boron atom in the *nido* face of the tungsten-ligating $\eta^5\text{-}C_2B_9H_9Me_2$ group. The other unit in the crystal exhibited disorder. This arises from its correspondence to the two products (**3e**) and (**3f**), which differ only in the occupancy [R = H (20%) or Et (80%)] of the *exo*-polyhedral site at the central boron in the C_2B_3 *nido* face of the carbaborane ligand. The structures of (**3e**) and (**3f**), with their *exo*-polyhedral B–Pt σ bonds and tungsten-ligated $\eta^5\text{-}C_2B_9H_7(R)Me_2$ groups are thus closely related to that of (**3a**). Protonation ($HBF_4\cdot Et_2O$) of the complexes (**3**) (L = PMe_3, CO, or $CNBu^t$) affords the salts $[PtW(\mu\text{-}H)(CO)_2(L)(PEt_3)_2\{\eta^5\text{-}C_2B_9H_8(CH_2C_6H_4Me\text{-}4)Me_2\}][BF_4]$. The n.m.r. data ($^1H$, $^{13}C\text{-}\{^1H\}$, $^{11}B\text{-}\{^1H\}$, and $^{31}P\text{-}\{^1H\}$) for the new compounds are reported, and are discussed in relation to their structures.

In a series of recent articles[1,2] we have reported studies on reactions between various low-valent metal complexes and the salts $[X][W(\equiv CR)(CO)_2(\eta^5\text{-}C_2B_9H_9Me_2)]$ [X = $N(PPh_3)_2$, NEt_4, $P(CH_2Ph)Ph_3$, or PPh_4; R = C_6H_4Me-4 or Me]. Initially these investigations arose through a recognition of the isolobal relationship between the anions $[W(\equiv CR)(CO)_2(\eta^5\text{-}C_2B_9H_9Me_2)]^-$ and the neutral compounds $[W(\equiv CR)(CO)_2(\eta\text{-}C_5H_5)]$, both types of species being formally electronically equivalent to an alkyne.[3,4] Thus as a consequence of the ligating properties of the W≡C group, reactions between the salts $[N(PPh_3)_2][W(\equiv CR)(CO)_2(\eta^5\text{-}C_2B_9H_9Me_2)]$ [(**1a**), R = C_6-

* Part 65 is the preceding paper.

† Di-μ-carbonyl-2-[3′,7′–11′-η-octahydro-7′,8′-dimethyl-10′-*p*-tolylmethyl-7′,8′-dicarba-*nido*-undecaborato(2−)]-1,1-bis(triethylphosphine)platinumtungsten (*Pt=W*)—dichloromethane(1/1) and 2,2-dicarbonyl-μ-[σ:7′–11′-η-heptahydro-7′,8′-dimethyl-10′-*p*-tolylmethyl-7′,8′-dicarba-*nido*-undecaborato(3−)-$C^{7',8'}$, $B^{9'-11'}$ (W), $B^{9'}$ (Pt)]-μ-hydrido-1,1-bis(triethylphosphine)-2-(trimethylphosphine)platinum-tungsten (*Pt–W*).

Supplementary data available: see Instructions for Authors, *J. Chem. Soc., Dalton Trans.*, 1987, Issue 1, pp. xvii—xix.

Non-S.I. unit employed: atm = 101 325 Pa.

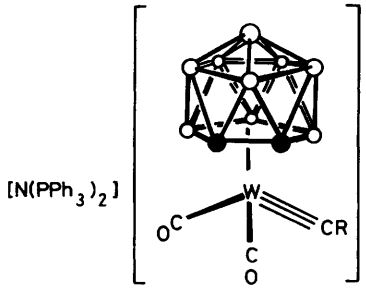

R

(**1a**) C_6H_4Me-4

(**1b**) Me

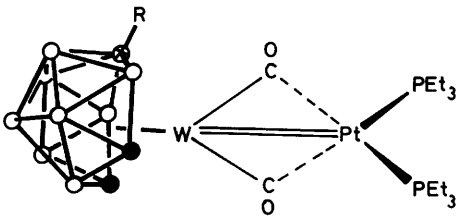

R

(**2a**) $CH_2C_6H_4Me$-4

(**2b**) H

(**2c**) Et

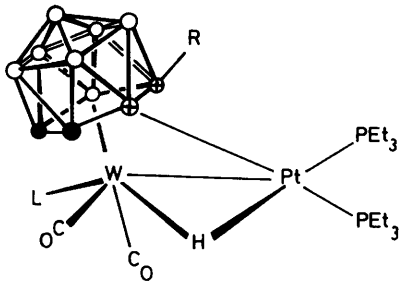

	R	L
(**3a**)	$CH_2C_6H_4Me$-4	PMe_3
(**3b**)	$CH_2C_6H_4Me$-4	CO
(**3c**)	$CH_2C_6H_4Me$-4	$CNBu^t$
(**3d**)	$CH_2C_6H_4Me$-4	$PHPh_2$
(**3e**)	H	CO
(**3f**)	Et	CO

○ BH ● CMe ⊕ B

H_4Me-4; (**1b**), R = Me] and the complex halide $[RhCl(PPh_3)_3]$ afford the dinuclear metal compounds $[RhW(\mu\text{-}CR)(CO)_2(PPh_3)_2(\eta^5\text{-}C_2B_9H_9Me_2)]$. The salt (**1a**) also reacts with cationic complexes such as $[Ru(CO)(NCMe)_2(\eta\text{-}C_5H_5)][BF_4]$ or $[M(CO)_2(NCMe)_2(\eta^5\text{-}C_9H_7)][BF_4]$ (M = Mo or W; $\eta^5\text{-}C_9H_7$ = indenyl), to give products with heteronuclear metal–metal bonds spanned by the *p*-tolylmethylidyne group.

A particularly interesting feature of this chemistry was the discovery of the non-spectator role of the $\eta^5\text{-}C_2B_9H_9Me_2$ ligand in several of the products. Thus in the complexes $[RuW(\mu\text{-}CC_6H_4Me\text{-}4)(CO)_3(\eta\text{-}C_5H_5)(\eta^5\text{-}C_2B_9H_9Me_2)]$ and $[MW(\mu\text{-}CC_6H_4Me\text{-}4)(CO)_3(\eta^5\text{-}C_9H_7)(\eta^5\text{-}C_2B_9H_9Me_2)]$ (M = Mo or W) obtained from the above mentioned cationic ruthenium, molybdenum, and tungsten species, although the carbaborane group remains pentahapto bonded to tungsten it also partakes in an *exo*-polyhedral three-centre two-electron B–H → M (M = Ru, Mo, or W) interaction, employing a BH fragment located in the *nido* face of the ligand.[2b,c] Moreover, in some reactions other groups which are present become linked to the C_2B_9 cage. Thus treatment of the rhodium compound $[Rh(PPh_3)_2(nbd)][PF_6]$ [nbd = norborna-2,5-diene (bicyclo-[2.2.1]hepta-2,5-diene)] with (**1a**) affords a product $[RhW(\mu\text{-}CC_6H_4Me\text{-}4)(CO)_2(PPh_3)_2\{\eta^5\text{-}C_2B_9H_8(C_7H_9)Me_2\}]$ with a C_7H_9 fragment, derived from nbd, attached to a boron atom in the open face of the cage.[2a]

In this paper we describe reactions between the salts (**1**) and the platinum complex $[PtH(Me_2CO)(PEt_3)_2][BF_4]$. It was anticipated that the reactive hydrido ligand present in the platinum compound would migrate to the alkylidyne groups in (**1**).[5] This would produce neutral complexes in which the Pt–W bonds would be bridged by alkylidene ligands CHR (R = C_6H_4Me-4 or Me). However, it was also expected that such systems if formed would be electronically unsaturated, and might undergo further reaction, leading to insertion of the alkylidene fragment into the carbaborane cage. We have previously shown that the alkylidyne group present in the complex $[MoW(\mu\text{-}CC_6H_4Me\text{-}4)(CO)_3(\eta^5\text{-}C_9H_7)(\eta^5\text{-}C_2B_9H_9Me_2)]$ inserts into a B–H bond in the open face of the carbaborane ligand on treatment of the molybdenum–tungsten compound with hex-3-yne.[6] A preliminary account of some of the results reported herein has been given.[7]

Results and Discussion

The reaction between $[PtH(Me_2CO)(PEt_3)_2][BF_4]$ and (**1a**) in acetone at *ca.* −30 °C affords the orange crystalline compound $[PtW(CO)_2(PEt_3)_2\{\eta^6\text{-}C_2B_9H_8(CH_2C_6H_4Me\text{-}4)Me_2\}]$ (**2a**), microanalytical and spectroscopic data for which are given in Tables 1—3. However, the structure of (**2a**) was not established until the results of an *X*-ray diffraction study became known. The molecule is shown in Figure 1, and selected bond distances and angles are given in Table 4.

In (**2a**) the Pt–W bond [2.602(1) Å] is semi-bridged by two CO groups [W–C(3)–O(3) 168(1), W–C(4)–O(4) 165(1)°]. The metal–metal distance is short, and is identical with that found in the salt $[PtW(CO)_2(PEt_3)_2(\eta\text{-}C_2H_4)(\eta\text{-}C_5H_5)][BF_4]$, for which a Pt=W bond has been invoked.[8] Typically Pt–W single bonds are in the range *ca.* 2.751—2.895 Å.[9] The two semi-

Table 1. Analytical[a] and physical data for the platinum–tungsten complexes

Compound[b]	Yield (%)	$\nu_{max.}$(BH)[c]/ cm^{-1}	$\nu_{max.}$(CO)[c]/ cm^{-1}	Analysis (%) C	H
(2a) $[PtW(CO)_2(PEt_3)_2\{\eta^6\text{-}C_2B_9H_8(CH_2C_6H_4Me\text{-}4)Me_2\}]$	80	2 546m	1 828s	32.7 (33.4)	5.2 (5.7)
(2b) $[PtW(CO)_2(PEt_3)_2(\eta^6\text{-}C_2B_9H_9Me_2)]$ } [d]	34	2 536m	1 875w, 1 831s	27.0 (27.0)	5.7 (5.6)
(2c) $[PtW(CO)_2(PEt_3)_2\{\eta^6\text{-}C_2B_9H_8(Et)Me_2\}]$ } [d]					
(3a) $[PtW(\mu\text{-}H)\{\mu\text{-}\sigma\text{:}\eta^5\text{-}C_2B_9H_7(CH_2C_6H_4Me\text{-}4)Me_2\}(CO)_2(PMe_3)(PEt_3)_2]$	81	2 550w	1 912m, 1 823s	34.4 (34.3)	6.3 (6.2)
(3b) $[PtW(\mu\text{-}H)\{\mu\text{-}\sigma\text{:}\eta^5\text{-}C_2B_9H_7(CH_2C_6H_4Me\text{-}4)Me_2\}(CO)_3(PEt_3)_2]$	90	2 539w	2 012s, 1 939m, 1 898m	33.4 (33.6)	5.2 (5.5)
(3c) $[PtW(\mu\text{-}H)\{\mu\text{-}\sigma\text{:}\eta^5\text{-}C_2B_9H_7(CH_2C_6H_4Me\text{-}4)Me_2\}(CO)_2(CNBu^t)(PEt_3)_2]$	46	2 550m	[e] 1 944m, 1 860s	[f] 37.3 (36.7)	6.4 (6.1)
(3d) $[PtW(\mu\text{-}H)\{\mu\text{-}\sigma\text{:}\eta^5\text{-}C_2B_9H_7(CH_2C_6H_4Me\text{-}4)Me_2\}(CO)_2(PHPh_2)(PEt_3)_2]$	64	2 553w	1 922m, 1 829s	41.7 (40.7)	5.8 (5.7)
(3e) $[PtW(\mu\text{-}H)(\mu\text{-}\sigma\text{:}\eta^5\text{-}C_2B_9H_8Me_2)(CO)_3(PEt_3)_2]$ } [g]	100	2 536m	2 013s, 1 950s, 1 940 (sh), 1 902m, 1 860 (sh), 1 850m	28.1 (27.5)	4.4 (4.6)
(3f) $[PtW(\mu\text{-}H)\{\mu\text{-}\sigma\text{:}\eta^5\text{-}C_2B_9H_7(Et)Me_2\}(CO)_3(PEt_3)_2]$ } [g]					
(4) $[PtW(CO)_3(PEt_3)_2(\eta^5\text{-}C_2B_9H_9Me_2)]$ } [g]					
(5a) $[PtW(\mu\text{-}H)(CO)_2(PMe_3)(PEt_3)_2\{\eta^5\text{-}C_2B_9H_8(CH_2C_6H_4Me\text{-}4)Me_2\}][BF_4]$	85	2 566m	1 938m, 1 854s	31.7 (31.7)	5.9 (5.8)
(5b) $[PtW(\mu\text{-}H)(CO)_3(PEt_3)_2\{\eta^5\text{-}C_2B_9H_8(CH_2C_6H_4Me\text{-}4)Me_2\}][BF_4]$	60	2 576m	2 039s, 1 975m, 1 927s	30.2 (30.8)	5.2 (5.2)
(5c) $[PtW(\mu\text{-}H)(CO)_2(CNBu^t)(PEt_3)_2\{\eta^5\text{-}C_2B_9H_8(CH_2C_6H_4Me\text{-}4)Me_2\}][BF_4]$	85	2 562m	[h] 1 972m, 1 893s	[i] 32.6 (33.6)	5.6 (5.7)

[a] Calculated values are given in parentheses. [b] Complexes or mixtures of complexes (see text) range from pale to dark orange in colour. [c] In CH_2Cl_2. [d] Inseparable mixture [(**2b**):(**2c**), 1:2] (see text), data refer to mixture. [e] $\nu_{max.}$(NC) at 2 131m cm^{-1}. [f] N, 1.6 (1.4%). [g] Data refer to (**3e**):(**3f**):(**4**) mixture (1 : 4 : 1), see text. [h] ν_{max}(NC) at 2 165m cm^{-1}. [i] N, 1.2 (1.3%).

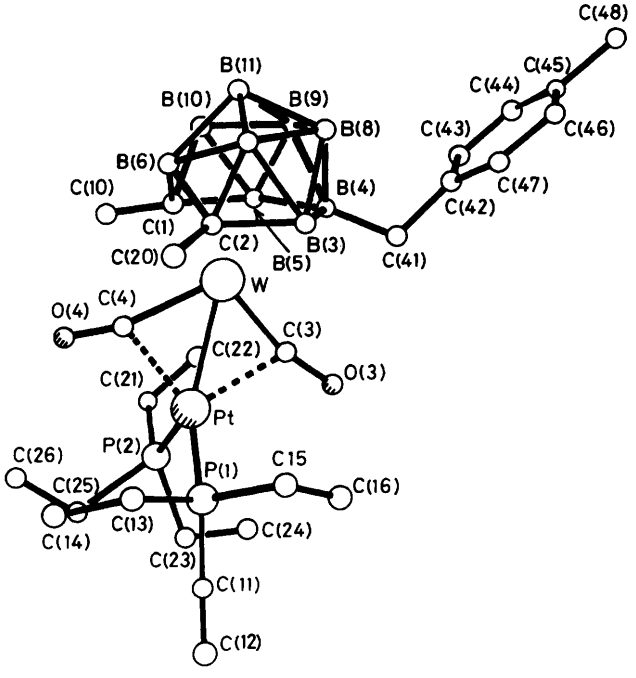

Figure 1. The molecular structure of $[PtW(CO)_2(PEt_3)_2\{\eta^6\text{-}C_2B_9H_8(CH_2C_6H_4Me\text{-}4)Me_2\}]$ (**2a**) showing the atom-labelling scheme

bridging carbonyl ligands and the metal atoms are essentially coplanar, and this plane is at 87° with respect to that defined by the PtP_2 group [P(1)–Pt–P(2) 106.9(2)°].

A novel feature of the structure relates to the carbaborane ligand attached to the tungsten, which has undergone substantial modification from its form in (**1a**). It now carries a $CH_2C_6H_4Me$-4 substituent at B(4), evidently derived from the terminal *p*-tolylmethylidyne group present in (**1a**), the hydrido ligand of $[PtH(Me_2CO)(PEt_3)_2]^+$, and the B(4)–H hydrogen atom of (**1a**). Evidence for this supposition will be given below. Although the two hydrogen atoms attached to C(41) were not located in the *X*-ray diffraction study, their presence was clearly revealed by ^1H n.m.r. spectroscopy. Moreover, the B(4)–C(41)–C(42) angle [117(1)°] and B(4)–C(41) separation [1.59(3) Å] correlate with sp^3 hybridisation at C(41).

A most significant result relates to the C_2B_9W cage, which no longer exhibits the *closo* icosahedral geometry present in the anion of (**1a**).[1] The C(1)–C(2) separation (2.88 Å) is non-bonding, and the tungsten atom is ligated by all six of the atoms C(1), C(2), B(3), B(4), B(5), and B(6), although not surprisingly W–B(4) [2.40(2) Å] and W–B(6) [2.51(2) Å] are distinctly longer than the connectivities W–B(3), W–B(5) [2.33(2) Å], W–C(1) [2.02(2) Å], and W–C(2) [2.04(2) Å]. The C_2B_9W cage geometry in (**2a**) is thus derived by scission of the C(1)–C(2) bond in (**1a**), with concomitant movement of B(6) towards the tungsten atom. This results in distortions within the cage structure, so that connectivities from the six-co-ordinated B(6) atom to its three boron nearest neighbours are relatively long (1.93—1.95 Å). The atoms C(1), C(2), B(3), B(4), and B(5) are essentially co-planar, and this plane is inclined at 24.5° to that defined by C(1), C(2), and B(6). The Pt–W vector lies at 13.7° to the normal to the plane defined by C(1), C(2), B(3), B(4), and B(5). The latter plane is inclined at 3.1° to that containing the essentially co-planar atoms B(7), B(8), B(9), and B(10). There is an approximate plane of symmetry in the molecule which is defined by the atoms Pt, W, C(3), C(4), B(4), B(6), B(11), and C(41). This feature is reflected in the n.m.r. data for (**2a**), discussed below.

Table 2. Hydrogen-1 and carbon-13 n.m.r. data[a] for the platinum–tungsten compounds

Compound	$^1H(\delta)$[b,c]	$^{13}C(\delta)$[d]
(2a)	1.09 [d of t, 18 H, $P(CH_2Me)_3$, *J*(HH) 8, *J*(PH) 17], 1.84 [m, 12 H, $P(CH_2Me)_3$], 2.28 (s, 3 H, Me-4), 2.35 (s, 6 H, CMe), 3.03 (s, 2 H, $BCH_2C_6H_4Me$-4), 6.91, 6.95 [$(AB)_2$, 4 H, C_6H_4, *J*(AB) 8]	[e] 243.8 [CO, *J*(WC) 160], 235.1 [CO, *J*(WC) 137], 176.6 (*C*Me), 144.0 [$C^1(C_6H_4)$], 131.6, 128.6, 127.3 (C_6H_4), 36.8 (br, $BCH_2C_6H_4Me$-4), 35.6 (*C*Me), 20.0 [m, $P(CH_2Me)_3$, Me-4], 7.8 [m, $P(CH_2Me)_3$]
(2b), **(2c)** } *f*,*g*	0.86 [t, BCH_2Me, *J*(HH) 8], 1.02 [m, $P(CH_2Me)_3$], 1.53 [q, BCH_2Me, *J*(HH) 8], 1.75 [m, $P(CH_2Me)_3$], 2.30* (s, CMe), 2.32 (s, CMe)	244.5* (CO), 243.8 (CO), 234.5* (CO), 232.3 [CO, *J*(WC) 177], 180.1 (*C*Me), 176.6* (*C*Me), 36.2 (*C*Me), 36.0* (*C*Me), 20.4 [m, $P(CH_2Me)_3$], 14.0 (BCH_2Me), 8.0 [m, $P(CH_2Me)_3$]
(3a)	−8.45 [d of d of d, 1 H, μ-H, *J*(PH) 55, 13, 10, *J*(PtH) 460, *J*(WH) 45], 1.11 [m, 18 H, $P(CH_2Me)_3$], 1.80 [d, 9 H, PMe_3, *J*(PH) 9], 1.96 [m, 13 H, $P(CH_2Me)_3$, $BCH_2C_6H_4Me$-4], 2.20, 2.21, 2.37 (s × 3, 9 H, CMe, Me-4), 2.62 [d, br, 1 H, $BCH_2C_6H_4Me$-4, *J*(HH) 15], 6.84, 6.89 [$(AB)_2$, 4 H, C_6H_4, *J*(AB) 8]	[e] 232.0 [d, CO, *J*(PC) 19, *J*(WC) 138], 224.2 [d, CO, *J*(PC) 21, *J*(WC) 147], 145.9 [$C^1(C_6H_4)$], 131.1, 127.7, 127.1 (C_6H_4), 62.2 (*C*Me), 60.1 [*C*Me, *J*(PtC) 30], 38.4 [*C*Me, *J*(PtC) 43], 31.8 (br, $BCH_2C_6H_4Me$-4), 30.3 (*C*Me), 20.3 (Me-4), 18.4, 16.6 [m × 2, $P(CH_2Me)_3$], 8.2, 7.8 [$P(CH_2Me)_3$]
(3b)	−8.81 [d of d, 1 H, μ-H, *J*(PH) 51, 16, *J*(PtH) 384, *J*(WH) 42], 1.12 [m, 18 H, $P(CH_2Me)_3$], 2.07 [m, 13 H, $P(CH_2Me)_3$, $BCH_2C_6H_4Me$-4], 2.22, 2.24, 2.34 (s × 3, 9 H, CMe, Me-4), 2.47 [d, br, 1 H, $BCH_2C_6H_4Me$-4, *J*(HH) 13], 6.88, 6.92 [$(AB)_2$, 4 H, C_6H_4, *J*(AB) 8]	[e] 223.7 [CO, *J*(WC) 116], 218.3 [CO, *J*(WC) 135], 214.0 [CO, *J*(PtC) 43, *J*(WC) 141], 143.6 [$C^1(C_6H_4)$], 131.9, 128.5, 127.5 (C_6H_4), 66.3 (*C*Me), 62.8 [*C*Me, *J*(PtC) 37], 36.5 [*C*Me, *J*(PtC) 37], 33.3 (br, $BCH_2C_6H_4Me$-4), 32.1 (*C*Me), 20.5 (Me-4), 18.9, 16.9 [m × 2, $P(CH_2Me)_3$], 8.4, 8.0 [$P(CH_2Me)_3$]
(3c)	−8.72 [d of d, 1 H, μ-H, *J*(PH) 57, 15, *J*(PtH) 435, *J*(WH) 42], 1.10 [m, 18 H, $P(CH_2Me)_3$], 1.52 (s, 9 H, Bu^t), 2.04 [m, 13 H, $P(CH_2Me)_3$, $BCH_2C_6H_4Me$-4], 2.18, 2.24, 2.32 (s × 3, 9 H, CMe, Me-4), 2.50 [d, br, 1 H, $BCH_2C_6H_4Me$-4, *J*(HH) 13], 6.91, 7.0 [$(AB)_2$, 4 H, C_6H_4, *J*(AB) 8]	[e] 225.1 [CO, *J*(WC) 135], 220.1 [CO, *J*(PtC) 46, *J*(WC) 128], 154.8 [*C*NBu^t, *J*(WC) 114], 144.1, 131.6, 128.8, 127.5 (C_6H_4), 63.2 (*C*Me), 61.9 [*C*Me, *J*(PtC) 33], 58.3 (Me_3CNC), 38.2 [*C*Me, *J*(PtC) 39], 33.5 (br, $BCH_2C_6H_4Me$-4), 31.0 (*C*Me), 30.2 (Me_3CNC), 20.6 (Me-4), 19.0, 16.7 [m × 2, $P(CH_2Me)_3$], 8.5, 8.0 [$P(CH_2Me)_3$]
(3d)	−8.29 [d of d of d, 1 H, μ-H, *J*(PH) 54, 13, 8, *J*(PtH) 442, *J*(WH) 43], 1.15 [m, 18 H, $P(CH_2Me)_3$], 1.48 (s, 3 H, CMe), 1.92—2.30 [m, 14 H, $P(CH_2Me)_3$, $BCH_2C_6H_4Me$-4], 2.35, 2.36 (s × 2, 6 H, CMe, Me-4), 5.29 [d, 1 H, $PHPh_2$ *J*(PH) 396], 6.98 (s, 4 H, C_6H_4), 7.32—7.71 (m, 10 H, Ph)	232.0 [d, CO, *J*(PC) 20], 221.0 [d, CO, *J*(PC) 17], 143.7—126.8 (Ph, C_6H_4), 62.3 (*C*Me), 61.0 [*C*Me, *J*(PtC) 34], 38.2 [*C*Me, *J*(PtC) 40], 32.0 [br, $BCH_2C_6H_4Me$-4], 27.4 (*C*Me), 19.9 (Me-4), 18.7, 16.5 [2 × m, $P(CH_2Me)_3$], 7.8, 7.4 [$P(CH_2Me)_3$]
(3e), **(3f)**, **(4)** } *h*	−9.12* [d of d, μ-H, *J*(PH) 51, 16, *J*(PtH) 376, *J*(WH) 42], −8.94† [d of d, μ-H, *J*(PH) 51, 15, *J*(PtH) 383, *J*(WH) 42], −7.06‡ [vbr, B(H)Pt, *J*PtH) *ca.* 500], 0.65—1.5, 1.9—2.4 (m × 2, PEt_3, CMe, Et)	231.5‡ [CO, *J*(PC) 5, *J*(PtC) 27, *J*(WC) 134], 224.9* [CO, *J*(WC) 117], 224.7† [CO, *J*(WC) 115], 222.7‡ [CO, *J*(PC) 7, *J*(PtC) 50, *J*(WC) 165], 220.4* [CO, *J*(PtC) 12, *J*(WC) 129], 219.4† [CO, *J*(PtC) 13, *J*(WC) 129], 215.3* [CO, *J*(PtC) 42, *J*(WC) 144], 213.8† [CO, *J*(PtC) 41, *J*(WC) 145], 67.6* (*C*Me), 66.2† (*C*Me), 63.8* [*C*Me, *J*(PtC) 34], 63.0† [*C*Me, *J*(PtC) 39], 62.6‡ (*C*Me), 36.9† [*C*Me, *J*(PtC) 34], 36.8* [*C*Me, *J*(PtC) 34], 32.4*† (*C*Me), 31.8‡ (*C*Me), 20.5—19.0, 17.5—16.5 [2 × m, $P(CH_2Me)_3$], 14.2† (BCH_2Me), 9.5—7.5 [m, $P(CH_2Me)_3$]
(5a)	−10.19 [d of d of d, 1 H, μ-H, *J*(PH) 56, 13, 10, *J*(PtH) 586, *J*(WH) 46], −5.4 [br, 1 H, B(μ-H)Pt, *J*(PtH) *ca.* 460], 1.25 [m, 18 H, $P(CH_2Me)_3$], 1.97 [d, 9 H, PMe_3, *J*(PH) 10], 2.25, 2.29 (s × 2, 6 H, CMe, Me-4), 2.38 [m, 16 H, $P(CH_2Me)_3$, CMe, $BCH_2C_6H_4Me$-4], 2.60 [d, 1 H, $BCH_2C_6H_4Me$-4, *J*(HH) 14], 6.75, 6.93 [$(AB)_2$, 4 H, C_6H_4, *J*(AB) 8]	226.8 [d, CO, *J*(PC) 24, *J*(PtC) 26], 223.3 [d, CO, *J*(PC) 24, *J*(PtC) 48], 142.7 [$C^1(C_6H_4)$], 132.4, 128.1, 127.4 (C_6H_4), 64.1, 59.7 (*C*Me), 38.6 [*C*Me, *J*(PtC) 21], 32.4 (br, $BCH_2C_6H_4Me$-4), 30.2 (*C*Me), 20.7 (Me-4), 19.0 [m, $P(CH_2Me)_3$], 16.5 [d, PMe_3, *J*(PC) 38], 16.6, 14.6 [$P(CH_2Me)_3$]
(5b)	−11.49 [d of d, 1 H, μ-H, *J*(PH) 53, 13, *J*(PtH) 580, *J*(WH) 40], −5.2 [br, 1 H, B(H)Pt, *J*(PtH) *ca.* 430], 1.31 [m, 18 H, $P(CH_2Me)_3$], 2.26, 2.34 (s × 2, 6 H, CMe, Me-4), 2.42 [m, 14 H, $P(CH_2Me)_3$, $BCH_2C_6H_4Me$-4], 2.52 (s, 3 H, CMe), 6.85, 6.98 [$(AB)_2$, 4 H, C_6H_4, *J*(AB) 8]	215.8, 215.2, 213.0 (CO), 141.2 [$C^1(C_6H_4)$], 133.4, 128.5, 128.0 (C_6H_4), 69.6, 62.6 (*C*Me), 37.1 [*C*Me, *J*(PtC) 20], 32.9 [br, $BCH_2C_6H_4Me$-4), 32.5 (*C*Me), 21.0 (Me-4), 19.6 [m, $P(CH_2Me)_3$], 9.0 [$P(CH_2Me)_3$]
(5c)	−10.78 [d of d, 1 H, μ-H, *J*(PH) 58, 13, *J*(PtH) 605, *J*(WH) 41], −5.5 [br, 1 H, B(H)Pt, *J*(PtH) *ca.* 440], 1.28 [m, 18 H, $P(CH_2Me)_3$], 1.57 (s, 9 H, Bu^t), 2.26, 2.31 (s × 2, 6 H, CMe, Me-4), 2.38 (s, 3 H, CMe), 2.45 [m, 14 H, $P(CH_2Me)_3$, $BCH_2C_6H_4Me$-4], 6.97 (s, 4 H, C_6H_4)	222.1, 219.6 (CO), 144.9 (*C*NBu^t), 142.4 [$C^1(C_6H_4)$], 133.6, 129.4, 128.6 (C_6H_4), 66.4, 60.8 (*C*Me), 54.8 (CMe_3), 38.5 (*C*Me), 34.0 (br, $BCH_2C_6H_4Me$-4), 31.6 (*C*Me), 30.4 (CMe_3), 21.0 (Me-4), 19.5 [m, $P(CH_2Me)_3$], 8.9, 8.8 [$P(CH_2Me)_3$]

[a] Chemical shifts (δ) in p.p.m., coupling constants in Hz, measurements at room temperature unless otherwise stated. [b] Measured in CD_2Cl_2. [c] Proton resonances for BH groups occur as broad unresolved signals in the range δ 0—3 p.p.m. [d] Hydrogen-1 decoupled, chemical shifts are positive to high frequency of $SiMe_4$, with measurements in CD_2Cl_2–CH_2Cl_2. [e] Measured at −40 °C. [f] Measured at −35 °C. [g] Data are for product mixture, integrals in ^1H spectrum not recorded. Peaks marked with asterisk due solely to complex **(2b)**, the minor product. [h] Data are for product mixture, peaks due solely to (**3e**), (**3f**), or (**4**) are labelled *, †, or ‡, respectively. Integrals in ^1H spectrum not recorded.

The results of the structural study show that (**2a**) must be classified as either an *iso-closo*[10,11] or a *hyper-closo* carbametallaborane.[12,13] Assuming a Pt=W bond, the platinum atom may be assigned a 16-electron valence shell. The interaction of the $W(CO)_2Pt(PEt_3)_2$ fragment with the cage ligand *via* the tungsten centre may be regarded in different ways. If the tungsten is considered to have an 18-valence electron configuration the C_2B_9W framework cannot be described as *closo*, *i.e.* with the metal contributing three orbitals for cage bonding in a 12-vertex system having 13 skeletal electron pairs. This classification is also ruled out on the grounds of the non-icosahedral geometry of the C_2B_9W cluster. There are two alternative descriptions[10–13] and each has aspects to commend it, but clearly further theoretical treatments are warranted.[14]

Employing the *hyper-closo* model for (**2a**), the $W(CO)_2Pt(PEt_3)_2$ fragment would contribute three orbitals and no electrons to the cage *via* the tungsten centre. The latter (W^0, d^6) would have an 18-electron valence shell, and be associated with

Table 3. Boron-11 and phosphorus-31 n.m.r. data[a] for the platinum–tungsten compounds

Compound	$^{11}B(\delta)$[b]	$^{31}P(\delta)$[c]
(**2a**)	28.9 (1 B, $BCH_2C_6H_4Me$-4), 15.0 (2 B), 0.9 (2 B), −3.3 (2 B), −20.3 (1 B), −27.3 (1 B)	35.7 [*J*(PtP) 3 347]
(**2b**), (**2c**)[d]	[e] 30.3 (BEt), 17.2, 14.0, −0.6, −3.9, −5.4, −20.5, −27.8	36.4 [*J*(PtP) 3 313], [f] 35.6 [*J*(PtP) 3 325]
(**3a**)	36.2 [1 B, BPt, *J*(PtB) *ca.* 400], 10.6 (1 B, $BCH_2C_6H_4Me$-4), −2.2 (1 B), −10.6 (br, 6 B)	23.2 [d of d, PEt_3, *J*(PP) 16, 8, *J*(PtP) 4 238], 13.7 [vbr, PEt_3, *J*(PtP) *ca.* 1 800], −18.3 [app. t, PMe_3, *J*(PP) 8, 8, *J*(PtP) 46, *J*(WP) 204]
(**3b**)	44.0 [1 B, BPt, *J*(PtB) *ca.* 420], 13.7 (1 B, $BCH_2C_6H_4Me$-4), 4.3 (1 B), −4.4 (6 B)	20.7 [d, *J*(PP) 17, *J*(PtP) 4 129], 13.5 [vbr, *J*(PtP) *ca.* 1 730]
(**3c**)	41.2 [1 B, BPt, *J*(PtB) *ca.* 440], 11.3 (1 B, $BCH_2C_6H_4Me$-4), −1.7 (1 B), −9.6 (6 B)	21.1 [d, *J*(PP) 17, *J*(PtP) 4 109], 14.5 [vbr, *J*(PtP) *ca.* 1 900]
(**3d**)	36.6 [1 B, BPt, *J*(PtB) *ca.* 480], 11.3 (1 B, $BCH_2C_6H_4Me$-4), −0.3 (1 B), −8.2 (1 B), −11.0 (4 B), −16.8 (1 B)	23.9 [d of d, PEt_3, *J*(PP) 16, 7, *J*(PtP) 4 240], 14.5 [vbr, PEt_3, *J*(PtP) *ca.* 1 800], 13.0 [app. t, $PHPh_2$, *J*(PP) 7, 7, *J*(PtP) 37, *J*(WP) 210]
(**3e**), (**3f**), (**4**)[g]	[e] 44.6† [BPt, *J*(PtB), *ca.* 500], 42.7* [BPt, *J*(PtB) *ca.* 500], 21.4‡ [B(μ-H)Pt, *J*(PtB) *ca.* 180], 14.7† (BEt), 2.4†, 1.0,*,‡ −0.2,*,‡ −7 to −17 (m, br)	20.6† [d, PEt_3, *J*(PP) 18, *J*(PtP) 4 118], 20.0* [d, PEt_3, *J*(PP) 18, *J*(PtP) 4 120], 14.6,*,† [vbr, PEt_3, *J*(PtP) *ca.* 1 800], 14.5‡ [d, PEt_3, *J*(PP) 22, *J*(PtP) 2 386], 9.0‡ [br, PEt_3, *J*(PtP) 3 776]
(**5a**)	12.6 [1 B, B(μ-H)Pt], 8.4 [1 B, $BCH_2C_6H_4Me$-4], −0.9 (1 B), −3.0 (1 B, BF_4), −10.5 (6 B)	23.7 [d of d, PEt_3, *J*(PP) 22, 8, *J*(PtP) 2 806], 15.0 [d, PEt_3, *J*(PP) 22, *J*(PtP) 3 178], −16.8 [d, PMe_3, *J*(PP) 8, *J*(PtP) 38, *J*(WP) 185]
(**5b**)	12.8 [2 B, B(μ-H)Pt, $BCH_2C_6H_4Me$-4], 2.3 (1 B), −2.8 (1 B, BF_4), −7.8 (6 B)	24.4 [d, *J*(PP) 17, *J*(PtP) 2 800], 18.3 [d, *J*(PP) 17, *J*(PtP) 3 070]
(**5c**)	9.1 [2 B, B(μ-H)Pt, $BCH_2C_6H_4Me$-4], −2.8 (1 B, BF_4), −8.4 (7 B)	23.1 [d, *J*(PP) 22, *J*(PtP) 2 754], 16.3 [d, *J*(PP) 22, *J*(PtP) 3 118]

[a] Chemical shifts (δ) in p.p.m., coupling constants in Hz, measurements in CD_2Cl_2–CH_2Cl_2 at ambient temperatures unless otherwise stated. [b] Hydrogen-1 decoupled, chemical shifts are positive to high frequency of BF_3·Et_2O (external). [c] Hydrogen-1 decoupled, chemical shifts are positive to high frequency of 85% H_3PO_4 (external). [d] Spectra of mixture (see text) measured at −40 °C. [e] Integrals not recorded. [f] Signal due to (**2b**). [g] Spectrum of mixture (see text), signals due to (**3e**), (**3f**), and (**4**) labelled *, †, and ‡ respectively.

Table 4. Selected internuclear distances (Å) and angles (°) for $[PtW(CO)_2(PEt_3)_2\{\eta^6\text{-}C_2B_9H_8(CH_2C_6H_4Me\text{-}4)Me_2\}]\cdot CH_2Cl_2$ (**2a**)

Pt–W	2.602(1)	Pt–P(1)	2.309(4)	Pt–P(2)	2.301(5)	W–C(3)	2.06(2)
W–C(4)	2.08(2)	C(3)–O(3)	1.19(2)	C(4)–O(4)	1.13(2)	Pt–C(3)	2.18(2)
Pt–C(4)	2.16(2)	W–C(1)	2.02(2)	W–C(2)	2.04(2)	W–B(3)	2.33(2)
W–B(4)	2.40(2)	W–B(5)	2.33(2)	W–B(6)	2.51(2)	C(1)–B(5)	1.66(3)
C(1)–B(6)	1.82(3)	C(1)–B(10)	1.62(3)	C(2)–B(3)	1.71(3)	C(2)–B(6)	1.78(3)
C(2)–B(7)	1.64(3)	B(3)–B(4)	1.78(3)	B(3)–B(7)	1.88(3)	B(3)–B(8)	1.88(3)
B(4)–B(5)	1.86(3)	B(4)–B(8)	1.86(3)	B(4)–B(9)	1.83(3)	B(5)–B(9)	1.79(3)
B(5)–B(10)	1.84(3)	B(6)–B(7)	1.95(3)	B(6)–B(10)	1.95(3)	B(6)–B(11)	1.93(3)
B(7)–B(8)	1.77(3)	B(7)–B(11)	1.81(3)	B(8)–B(9)	1.79(3)	B(8)–B(11)	1.81(3)
B(9)–B(10)	1.78(3)	B(9)–B(11)	1.75(3)	B(10)–B(11)	1.74(3)	B(4)–C(41)	1.59(3)
W–Pt–P(1)	125.2(1)	W–Pt–P(2)	127.8(1)	P(1)–Pt–P(2)	106.9(2)	W–C(3)–O(3)	168(1)
W–C(4)–O(4)	165(1)	Pt–C(3)–O(3)	117(1)	Pt–C(4)–O(4)	119(1)	C(3)–W–C(4)	107.8(6)
B(6)–C(2)–B(3)	110(1)	C(2)–B(3)–B(4)	115(1)	B(3)–B(4)–B(5)	121(1)	B(4)–B(5)–C(1)	115(1)
B(5)–C(1)–B(6)	109(1)	C(1)–B(6)–C(2)	106(1)	B(4)–C(41)–C(42)	117(1)		

a 12-vertex C_2B_9W cluster with 12 skeletal electron pairs. Alternatively, if the $W(CO)_2Pt(PEt_3)_2$ unit contributes four valence orbitals and two electrons (W^{II}, d^4) to the cage, the tungsten retains its 18-electron valence shell but it is associated with a 12-vertex C_2B_9W cluster with 13 skeletal electron pairs. This is consistent with the *iso-closo* model, as is the core geometry which may be visualised as a capping of a C_2B_9 *arachno* structure by the metal vertex, resulting in a closed deltahedral form.[10,11]

A theoretical analysis of some metallaborane cage structures supports the *hyper-closo versus iso-closo* model.[14] However, this treatment considered deltahedra containing a unique high-connectivity vertex on the principal axis. Compound (**2a**) has two high connectivity sites [W and B(6)], but these are not located on a principal axis, a structural feature which is absent. However, if the presence of the substituent on B(4) and the difference between the B(6) and W centres is ignored, there is an approximate C_{2v} axis through the mid-points of B(8)–B(9) and C(1)···C(2). Compound (**2a**) appears to be the first example of a structurally characterised 12-vertex cage system necessitating modification of the classical skeletal electron pair theory. Moreover, it is one involving a transition element known to prefer in its organo-ligand complexes an 18- rather than a 16-electron valence shell.

Structurally the $(OC)_2W{=}Pt(PEt_3)_2$ fragment in (**2a**) is similar to that in the complex $[PtW(CO)_2(PEt_3)_2(\eta\text{-}C_2H_4)(\eta\text{-}C_5H_5)][BF_4]$,[8] which also has an electronically unsaturated tungsten centre. There is, however, an important symmetry difference between the two species. In both complexes the plane defined by the semi-bridging carbonyl groups and the metal atoms is essentially orthogonal to that defined by the PtP_2 atoms. However, in (**2a**) the metal atoms and carbonyl ligands

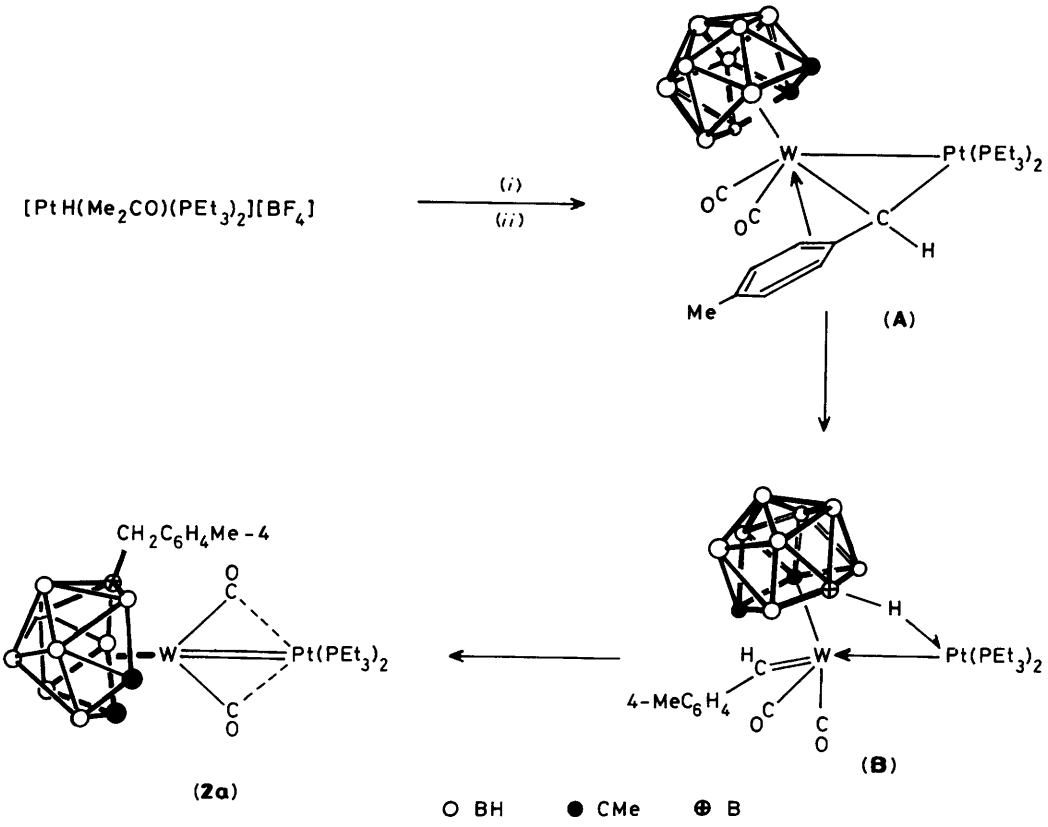

Scheme 1. (*i*) $+[N(PPh_3)_2][W(\equiv CC_6H_4Me\text{-}4)(CO)_2(\eta^5\text{-}C_2B_9H_9Me_2)]$, (*ii*) $-[N(PPh_3)_2][BF_4]$ and Me_2CO

lie in the molecular symmetry plane, whereas in the cation of $[PtW(CO)_2(PEt_3)_2(\eta\text{-}C_2H_4)(\eta\text{-}C_5H_5)][BF_4]$ it is the phosphorus atoms and the metal atoms which lie in the plane of symmetry. This difference would seem to inject a note of caution in comparisons of the bonding in the two species.

Having established the structure of (**2a**) by *X*-ray diffraction, it is possible to interpret the spectroscopic data (Tables 1—3). The presence of the semi-bridging carbonyl groups is revealed by the observation of a single CO stretching band at 1 828 cm^{-1}. The $^{13}C\text{-}\{^1H\}$ n.m.r. spectrum shows characteristic resonances for these chemically distinct ligands at δ 235.1 and 243.8 p.p.m. with $^{183}W\text{–}^{13}C$ couplings (Table 2). In the $^{13}C\text{-}\{^1H\}$ n.m.r. spectrum of the compound $[PtW(CO)_2(PEt_3)_2(\eta\text{-}C_2H_4)(\eta\text{-}C_5H_5)][BF_4]$, where the CO groups lie symmetrically above and below the symmetry plane, there is one resonance for these ligands (δ 237.5 p.p.m.).[8]

The presence of the plane of symmetry in (**2a**), defined above, results in the appearance of only one resonance for the two tungsten-ligated *C*Me nuclei, and this occurs at δ 176.6 p.p.m. This signal, which remains a singlet in a fully coupled spectrum, is substantially deshielded compared with the corresponding resonances observed for carbon nuclei in normal *closo* icosahedral metallacarbaboranes. Resonances for the latter appear near δ 60 p.p.m., *e.g.* for the compound $[NEt_4][PtW(\mu\text{-}CPh)(CO)_2(cod)(\eta^5\text{-}C_2B_9H_9Me_2)]$ (cod = cyclo-octa-1,5-diene) the signals for the *C*Me groups in the $^{13}C\text{-}\{^1H\}$ n.m.r. spectrum occur at δ 59.5 and 62.1 p.p.m.[1] A signal in the $^{13}C\text{-}\{^1H\}$ n.m.r. spectrum of (**2a**) at δ 36.8 p.p.m. is assigned to the $CH_2C_6H_4Me$-4 nucleus.

The appearance in the $^{11}B\text{-}\{^1H\}$ n.m.r. spectrum of (**2a**) of six peaks (Table 3) of relative intensity 1:1:2:2:2:1 is in accord with the mirror symmetry in the molecule. Assignment of the signal at 28.9 p.p.m. to the $BCH_2C_6H_4Me$-4 group is reasonable since in a fully proton-coupled spectrum this resonance shows no coupling. As expected, the $^{31}P\text{-}\{^1H\}$ n.m.r. spectrum shows one resonance at 35.7 p.p.m. with *J*(PtP) 3 347 Hz, a value typical for a $Pt(PEt_3)_2$ group.[8,15]

The reaction which affords (**2a**) has two unusual features, the generation of an *iso-closo* (or *hyper-closo*) cage structure, and the transformation of the *p*-tolylmethylidyne ligand in (**1a**) into the $CH_2C_6H_4Me$-4 substituent at B(4) (Figure 1). In order to confirm the involvement of the hydrido ligand in the precursor $[PtH(Me_2CO)(PEt_3)_2][BF_4]$ in the formation of the CH_2 group, the reaction between (**1a**) and $[PtD(Me_2CO)(PEt_3)_2][BF_4]$ was investigated, and the $^2H\text{-}\{^1H\}$ n.m.r. spectrum of the product recorded. This revealed a singlet signal at δ 3.0 for the $CD(H)C_6H_4Me$-4 group.

There are several possible pathways for the formation of (**2a**). We favour that shown in Scheme 1, since the $\mu\text{-}\sigma\text{:}\eta^3\text{-}C(H)C_6H_4Me$-4 ligand present in the intermediate (**A**) has been identified by *X*-ray diffraction in the complex $[PtW\{\mu\text{-}\sigma\text{:}\eta^3\text{-}C(H)C_6H_4Me\text{-}4\}(CO)_2(PMe_3)_2(\eta\text{-}C_5H_5)][BF_4]$.[16] Moreover, the reagent $[PtH(Me_2CO)(PEt_3)_2][BF_4]$ is known to react with $[W(\equiv CC_6H_4Me\text{-}4)(CO)_2(\eta\text{-}C_5H_5)]$ to give the closely related compound $[PtW\{\mu\text{-}\sigma\text{:}\eta^3\text{-}C(H)C_6H_4Me\text{-}4\}(CO)_2(PEt_3)_2(\eta\text{-}C_5H_5)][BF_4]$,[5] so that Pt–H addition to C≡W to give the $\sigma\text{:}\eta^3\text{-}C(H)C_6H_4Me$-4 group has precedent. The B–H → Pt bridge in the intermediate (**B**) is similar to other three-centre two-electron bonds identified previously.[2b,c] Conversion of (**B**) into (**2a**) involves hydroboration of the ligated alkylidene fragment by the platinum-activated BH group, with concomitant rupture of the C–C bond in the cage. Addition of B–H to unsaturated carbon–tungsten bonds has been previously observed.[17] When the preparation of (**2a**) was carried out at −78 °C a deep green intermediate was seen, but it could not be isolated since above *ca.* −50 °C it converted to the orange

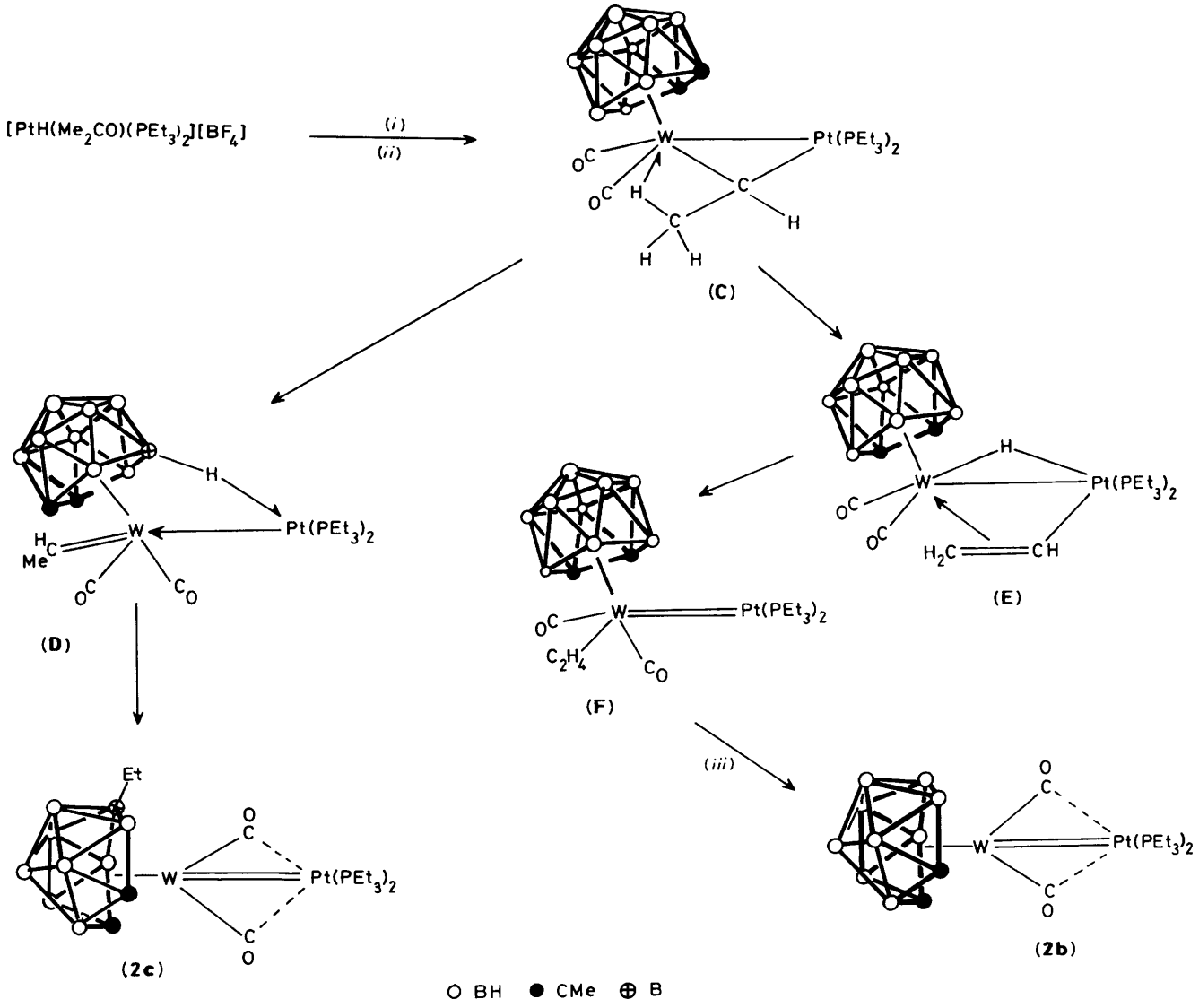

Scheme 2. (*i*) $+[N(PPh_3)_2][W(\equiv CMe)(CO)_2(\eta^5\text{-}C_2B_9H_9Me_2)]$, (*ii*) $-[N(PPh_3)_2][BF_4]$ and Me_2CO, (*iii*) $-C_2H_4$

species (**2a**). The cleavage of the C–C bond in the final step may take place in order to relieve electron deficiency at the tungsten atom. However, this process might occur earlier in the sequence.

The reaction between (**1b**) and $[PtH(Me_2CO)(PEt_3)_2][BF_4]$ was next investigated, since the presence of the methyl substituent on the alkylidyne carbon atom rather than a *p*-tolyl group has been shown to induce differences in reactivity, and sometimes affords different products.[8,18] The two reagents give an orange crystalline mixture of two compounds. Unfortunately, attempts to separate these products by fractional crystallisation or by column chromatography were unsuccessful. However, the spectroscopic data (Tables 1—3) unequivocally establish that the complexes formed are $[PtW(CO)_2(PEt_3)_2\{\eta^6\text{-}C_2B_9H_8(R)\text{-}Me_2\}]$ [(**2b**), R = H; (**2c**), R = Et], and from the peak intensities in the i.r. and ^1H n.m.r. spectra it was deduced that (**2b**) and (**2c**) were produced in the ratio 1:2.

The presence of the two closely related species was most clearly demonstrated in the $^{31}P\text{-}\{^1H\}$ n.m.r. spectrum (Table 3) which showed two signals with no mutual coupling, but with chemical shifts [δ 35.6 (**2b**), and 36.4 p.p.m. (**2c**)] and coupling constants [*J*(PtP) 3 325 (**2b**) and 3 313 Hz (**2c**)] similar to those for (**2a**) [δ 35.7 p.p.m., *J*(PtP) 3 347 Hz].

The ^1H n.m.r. spectrum of the mixture of (**2b**) and (**2c**) displayed two resonances [δ 2.30 (**2b**) and 2.32 (**2c**)] for the equivalent CMe groups present in the carbaborane cage in each species. The PEt_3 ligands give rise to two complex patterns in the ^1H spectrum, but fortunately these did not obscure the signals for the BEt group in (**2c**), seen as a triplet at δ 0.86 (Me) and a quartet at 1.53 (CH_2), with *J*(HH) 8 Hz. This assignment was confirmed by homonuclear decoupling. Moreover, the reaction between $[PtD(Me_2CO)(PEt_3)_2][BF_4]$ and (**1b**) afforded a product mixture, the $^2H\text{-}\{^1H\}$ n.m.r. spectrum of which showed one singlet resonance at δ 1.5.

The $^{13}C\text{-}\{^1H\}$ n.m.r. data (Table 2) are also readily understood as representing a mixture of (**2b**) and (**2c**). Good correlations exist between the chemical shifts observed and those in the $^{13}C\text{-}\{^1H\}$ n.m.r. spectrum of (**2a**). Thus resonances for the CO ligands of the minor product (**2b**) occur at δ 244.5 and 234.5 p.p.m., with those for (**2c**) at 243.8 and 232.3 p.p.m. The signals at δ 180.1 (**2c**) and 176.6 (**2b**) p.p.m. may likewise be assigned to the equivalent *C*Me groups in each species. A signal at δ 14.0 is attributed to the $BCH_2\mathit{Me}$ group in (**2c**) but the BCH_2Me resonance was not observed, due either to ^{11}B broadening, or overlap with peaks for the PEt_3 groups. In the

Table 5. Selected internuclear distances (Å) and angles (°) for $[PtW(\mu\text{-}H)\{\mu\text{-}\sigma\text{:}\eta^5\text{-}C_2B_9H_7(CH_2C_6H_4Me\text{-}4)Me_2\}(CO)_2(PMe_3)(PEt_3)_2]$ (**3a**)

Pt–W	2.843(2)	Pt–P(1)	2.370(2)	Pt–P(2)	2.254(3)	W–P(3)	2.481(2)
W–C(3)	1.976(5)	W–C(4)	1.977(6)	Pt–H(1)	1.88(6)	W–H(1)	1.53(5)
C(3)–O(3)	1.154(6)	C(4)–O(4)	1.142(8)	W–C(1)	2.424(5)	W–C(2)	2.345(5)
W–B(3)	2.269(6)	Pt–B(3)	2.123(5)	W–B(4)	2.421(6)	W–B(5)	2.405(5)
B(4)–C(41)	1.619(7)	C(1)–C(2)	1.620(7)	C(2)–B(3)	1.806(6)	B(3)–B(4)	1.850(8)
B(4)–B(5)	1.786(9)	B(5)–C(1)	1.743(7)				
W–Pt–P(1)	110.9(1)	W–Pt–P(2)	144.8(1)	W–Pt–B(3)	51.9(2)	W–Pt–H(1)	30(2)
P(1)–Pt–P(2)	103.8(1)	P(1)–Pt–H(1)	88(2)	P(1)–Pt–B(3)	162.1(2)	P(2)–Pt–H(1)	161(2)
P(2)–Pt–B(3)	93.9(2)	H(1)–Pt–B(3)	74(2)	Pt–W–H(1)	37(2)	W–H(1)–Pt	113(3)
H(1)–W–P(3)	130(2)	Pt–W–P(3)	144.4(1)	Pt–W–C(3)	70.5(2)	Pt–W–C(4)	102.9(2)
P(3)–W–C(3)	74.7(2)	P(3)–W–C(4)	77.1(2)	C(3)–W–C(4)	101.9(2)	W–C(3)–O(3)	174.5(4)
W–C(4)–O(4)	175.8(5)	C(1)–C(2)–B(3)	110.2(4)	C(2)–B(3)–B(4)	106.4(4)	B(3)–B(4)–B(5)	102.7(4)
B(4)–B(5)–C(1)	110.5(4)	C(2)–B(3)–Pt	110.8(3)	B(4)–B(3)–Pt	120.5(3)	W–B(3)–Pt	80.6(2)
B(4)–C(41)–C(42)	115.9(4)						

^{11}B-$\{^1H\}$ n.m.r. spectrum (Table 3) the low-field signal at δ 30.3 p.p.m. is as expected for a BEt group and, moreover, in a fully coupled spectrum this was the only peak which showed no ^1H coupling.

The two products (**2b**) and (**2c**) are formed in slightly different ratios depending on the reaction conditions (*ca.* −78 to −20 °C), with higher temperatures leading to other products including $[N(PPh_3)_2][7,8\text{-}C_2B_9H_{10}Me_2]$. It is likely that (**2c**) is formed *via* a mechanism similar to that which yields (**2a**). Moreover, in the formation of the former there is probably an intermediate which can isomerise and release ethylene, thereby providing a pathway to (**2b**). In Scheme 2 we indicate possible routes to (**2b**) and (**2c**). It is suggested that addition of the Pt–H group of $[PtH(Me_2CO)(PEt_3)_2][BF_4]$ to the W≡C bond of (**1b**) initially produces intermediate (**C**), in which an agostic C–H → W interaction allows the tungsten centre to adopt an 18-electron valence shell. The relationship between (**C**) of Scheme 2 and (**A**) of Scheme 1 is apparent. Moreover, the subsequent step to (**2c**) *via* (**D**) is analogous to the pathway to (**2a**) *via* (**B**) in Scheme 1. In Scheme 2 the alternative pathway (**C**) ⟶ (**E**) ⟶ (**F**) leads to complex (**2b**), the minor product of the reaction. Analogous transformations have been invoked in the synthesis of the ethylene complex $[PtW(CO)_2(PEt_3)_2(\eta\text{-}C_2H_4)(\eta\text{-}C_5H_5)][BF_4]$, obtained by treating $[PtW(\mu\text{-}CMe)(CO)_2(PEt_3)_2(\eta\text{-}C_5H_5)]$ with $HBF_4{\cdot}Et_2O$.[8] Also the preparation of the unsaturated dimetal complex $[RhW(CO)_3(PPh_3)_2(\eta\text{-}C_5H_5)]$ from the reaction between $[W(\equiv CMe)(CO)_2(\eta\text{-}C_5H_5)]$ and $[RhH(CO)(PPh_3)_3]$ involves a process in which ethylene is eliminated after combination of the ligands H and CMe.[18]

Since compound (**2a**) is a formally unsaturated dimetal species (30 valence electrons), it was anticipated that it would react with donor molecules. In such reactions it was important to establish whether the cage structure would change following relief of the electron deficiency at the tungsten centre. Treatment of CH_2Cl_2 solutions of (**2a**) with PMe_3, CO, $CNBu^t$, and $PHPh_2$ afforded the complexes $[PtW(\mu\text{-}H)\{\mu\text{-}\sigma\text{:}\eta^5\text{-}C_2B_9H_7(CH_2C_6H_4Me\text{-}4)Me_2\}(CO)_2(L)(PEt_3)_2]$ [(**3a**), L = PMe_3; (**3b**), L = CO; (**3c**), L = $CNBu^t$; (**3d**), L = $PHPh_2$], data for which are given in Tables 1—3. Perhaps surprisingly, (**2a**) does not react with ethylene. Interestingly, CH_2Cl_2 solutions of (**2a**) at room temperature slowly yield (**3b**) as a decomposition product. The reactions of (**2a**) with donor molecules parallel that between the 10-vertex carbametallaborane [*hyper-closo*-6,6-$(PEt_3)_2$-6,2,3-$RuC_2B_7H_9$] and PEt_3 which gives [*closo*-6,6,6-$(PEt_3)_3$-6,2,3-$RuC_2B_7H_9$].[12]

The spectroscopic data for the complexes (**3**) are in accord with the formulations proposed, but the structure of (**3a**) was unequivocally established by an *X*-ray diffraction study. The results are summarised in Table 5, and the structure is shown in Figure 2. The Pt–W bond [2.843(2) Å], appreciably longer than that in (**2a**), is bridged by a hydride ligand and by the cage system *via* an *exo*-polyhedral B–Pt bond [2.123(5) Å]. The hydrido ligand [H(1)] was located during refinement of the structure as the major remaining peak of electron density in an electron-density difference map after all other atoms were included, and its positional and thermal parameters were refined. However, the W–H(1) and Pt–H(1) separations (Table 5) deviate from those found by *X*-ray or neutron diffraction in other systems with bridging hydrides [typically W–H 1.88(1), Pt–H 1.78(5) Å].[19] Nevertheless, the results established the presence of the hydride, and the site found is in accord with that calculated using the steric-potential-energy-minimisation technique.[20]

The CO ligands attached to the tungsten are essentially terminally bound to this centre [W–C–O *ca.* 175°], and the tungsten carries the PMe_3 group at a distance [W–P(3) 2.481(2) Å] similar to that found [2.402(4) Å] in $[PtW\{\mu\text{-}C(C_6H_4Me\text{-}4)C(O)\}(CO)(PMe_3)(cod)(\eta\text{-}C_5H_5)]$.[21] The C_2B_9 carbaborane cage retains the $CH_2C_6H_4Me$-4 substituent, but has reverted to the *nido* icosahedral form, albeit slightly distorted, as a consequence of the addition of the electron pair donor (PMe_3). The C(1)–C(2) distance [1.620(7) Å] is now bonding.

The presence of the B(3)–Pt linkage results in a slippage of the tungsten from above the centroid of the B(6)B(7)B(8)B(9)B(10) ring towards B(3) by 0.18 Å. Connectivities to B(3) within the C_2B_3 η^5-ligated face are somewhat longer than comparable distances between other atoms [B(3)–B(4) 1.850(8), B(4)–B(5) 1.786(9), B(3)–C(2) 1.806(8), B(5)–C(1) 1.743(7) Å]. Ignoring μ-H(1), the atoms directly connected to platinum [W, B(3), P(1), and P(2)] are essentially co-planar, with B(3) *trans* and *cis* to P(1) and P(2), respectively [B(3)–Pt–P(1) 162.1(2), B(3)–Pt–P(2) 93.9(2), and P(1)–Pt–P(2) 103.8(1)°].

The spectroscopic data for (**3a**) are in complete agreement with the structure established by *X*-ray diffraction. In the i.r. spectrum there are two carbonyl stretching bands at 1 823 and 1 912 cm^{-1}. The ^1H n.m.r. spectrum (Table 2) showed a characteristic signal for the μ-H ligand at δ −8.45, with coupling to the three non-equivalent phosphorus nuclei, and with ^{195}Pt and ^{183}W satellite peaks. Unlike the situation with (**2a**), the CMe groups in (**3a**) are not equivalent. Consequently, in the ^{13}C-$\{^1H\}$ n.m.r. spectrum of the latter there are two *C*Me (δ 62.2 and 60.1 p.p.m.) and two C*Me* (δ 38.4 and 30.3 p.p.m.) signals. It is noteworthy that the *C*Me peaks are in the customary chemical shift range for such groups in an icosahedral MC_2B_9 (M = transition metal) structure, and this contrasts with the *C*Me shifts observed in the spectrum of (**2a**), discussed above. Also pertinent is the observation of ^{195}Pt–^{13}C coupling on the signals of one *C*Me [δ 60.1 p.p.m., *J*(PtC) 30 Hz] and one C*Me*

Table 6. Selected internuclear distances (Å) and angles (°) for $[PtW(\mu\text{-}H)(\mu\text{-}\sigma{:}\eta^5\text{-}C_2B_9H_8Me_2)(CO)_3(PEt_3)_2]$ (**3e**), $[PtW(\mu\text{-}H)\{\mu\text{-}\sigma{:}\eta^5\text{-}C_2B_9H_7(Et)Me_2\}(CO)_3(PEt_3)_2]$ (**3f**), and $[PtW(CO)_3(PEt_3)_2(\eta^5\text{-}C_2B_9H_9Me_2)]$ (**4**)

Molecule I (**3e**) and (**3f**)

Pt(1)–W(1)	2.902(1)	Pt(1)–P(11)	2.370(4)	Pt(1)–P(12)	2.260(4)	W(1)–C(14)	1.90(2)
W(1)–C(15)	1.93(2)	W(1)–C(16)	1.98(1)	Pt(1)–H(10)	2.2(1)	W(1)–H(10)	1.4(1)
C(14)–O(14)	1.18(2)	C(15)–O(15)	1.17(2)	C(16)–O(16)	1.14(2)	W(1)–C(11)	2.38(1)
W(1)–C(12)	2.40(1)	W(1)–B(13)	2.31(1)	Pt(1)–B(13)	2.15(2)	W(1)–B(14)	2.39(2)
W(1)–B(15)	2.38(2)	B(14)–C(140)	1.68(4)	C(140)–C(141)	1.40(5)	C(11)–C(12)	1.66(2)
C(12)–B(13)	1.76(2)	B(13)–B(14)	1.86(2)	B(14)–B(15)	1.78(2)	B(15)–C(11)	1.78(2)
W(1)–Pt(1)–P(11)	115.3(1)	W(1)–Pt(1)–P(12)	142.2(1)	W(1)–Pt(1)–B(13)	51.8(4)	W(1)–Pt(1)–H(10)	28(3)
P(11)–Pt(1)–P(12)	101.9(1)	P(11)–Pt(1)–H(10)	92(3)	P(11)–Pt(1)–B(13)	165.6(4)	P(12)–Pt(1)–H(10)	164(3)
P(12)–Pt(1)–B(13)	91.9(4)	H(10)–Pt(1)–B(13)	74(3)	Pt(1)–W(1)–H(10)	47(5)	W(1)–H(10)–Pt(1)	105(7)
Pt(1)–W(1)–C(14)	83.1(4)	Pt(1)–W(1)–C(15)	93.7(5)	Pt(1)–W(1)–C(16)	154.5(4)	C(14)–W(1)–C(15)	102.1(7)
C(15)–W(1)–C(16)	75.9(7)	C(16)–W(1)–C(14)	76.7(6)	W(1)–C(14)–O(14)	178(1)	W(1)–C(15)–O(15)	177(1)
W(1)–C(16)–O(16)	177(2)	C(11)–C(12)–B(13)	109(1)	C(12)–B(13)–B(14)	108(1)	B(13)–B(14)–B(15)	105(1)
B(14)–B(15)–C(11)	107(1)	C(12)–B(13)–Pt(1)	113.2(9)	B(14)–B(13)–Pt(1)	117(1)	W(1)–B(13)–Pt(1)	81.1(6)
B(14)–C(140)–C(141)	114(3)						

Molecule II (**4**)

Pt(2)–W(2)	2.818(1)	Pt(2)–P(21)	2.269(4)	Pt(2)–P(22)	2.311(3)	W(2)–C(24)	1.96(2)
W(2)–C(25)	1.94(2)	W(2)–C(26)	1.94(1)	C(24)–O(24)	1.17(2)	C(25)–O(25)	1.19(2)
C(26)–O(26)	1.17(2)	W(2)–C(21)	2.38(2)	W(2)–C(22)	2.38(2)	W(2)–B(23)	2.31(2)
W(2)–B(24)	2.32(2)	Pt(2)–B(24)	2.41(2)	W(2)–B(25)	2.34(2)	B(24)–H(24)	1.48(13)
Pt(2)–H(24)	1.06(13)	C(21)–C(22)	1.67(3)	C(22)–B(23)	1.68(3)	B(23)–B(24)	1.77(2)
B(24)–B(25)	1.96(3)	B(25)–C(21)	1.71(2)				
W(2)–Pt(2)–P(21)	106.6(1)	W(2)–Pt(2)–P(22)	156.4(1)	W(2)–Pt(2)–B(24)	51.9(4)		
P(21)–Pt(2)–P(22)	97.0(1)	P(21)–Pt(2)–H(24)	156(6)	P(21)–Pt(2)–B(24)	158.4(4)		
P(22)–Pt(2)–B(24)	104.5(4)	H(24)–Pt(2)–B(24)	21(7)	Pt(2)–W(2)–C(24)	76.7(4)	Pt(2)–W(2)–C(25)	76.1(4)
Pt(2)–W(2)–C(26)	139.8(5)	C(24)–W(2)–C(25)	103.1(6)	C(25)–W(2)–C(26)	78.3(6)	C(26)–W(2)–C(24)	79.5(7)
W(2)–C(24)–O(24)	176(1)	W(2)–C(25)–O(25)	172(1)	W(2)–C(26)–O(26)	177(1)	C(21)–C(22)–B(23)	112(1)
C(22)–B(23)–B(24)	104(1)	B(23)–B(24)–B(25)	109(1)	B(24)–B(25)–C(21)	105(1)	B(23)–B(24)–Pt(2)	109(1)
B(25)–B(24)–Pt(2)	108(1)						

nucleus [δ 38.4 p.p.m., J(PtC) 43 Hz]. We assign these couplings to C(1) and C(20) of Figure 2, respectively, on the basis that they are ^3J(PtC) values. This is consistent with the magnitude of such couplings varying in the sequence $^3J(PtC) > {}^2J(PtC) > {}^4J(PtC) \approx 0$ Hz.[22] Selective ^{195}Pt–^{13}C coupling to one *C*Me and one C*Me* group may well be structurally informative when comparing molecules with very similar structures, as discussed later. However, differences in the hybridisation of the atoms involved and the absence of σ bonds would effect the magnitude of the coupling. This is illustrated by the ^{13}C-{^{1}H} n.m.r. data for the anionic complexes $[PtW(\mu\text{-}CR)(CO)_2(cod)(\eta^5\text{-}C_2B_9H_9Me_2)]^-$ (R = C_6H_4Me-4 or Ph). The spectra of both these species each display two *C*Me and two C*Me* resonances.[1] As with (**3a**), in each spectrum only one *C*Me and one C*Me* signal shows ^{195}Pt–^{13}C coupling. For the *p*-tolylmethylidyne complex the data are δ(*C*Me) 72.8 p.p.m. with J(PtC) 142 Hz, and δ(C*Me*) 33.0 p.p.m. with J(PtC) 15 Hz. These couplings correspond, *via* the Pt–W bond, to ^2J(PtC) and ^3J(PtC) values. Moreover, the two-bond coupling is larger than the three-bond coupling which is perhaps a consequence of the π co-ordination of the cage ligand to the tungsten. More significantly, the anionic platinum–tungsten complexes, unlike (**3a**), do not have a direct σ bond between the platinum and the cage.

In the ^{1}H n.m.r. spectrum of (**3a**) only one part of the AB pattern for the diastereotopic methylene group $BCH_2C_6H_4$Me-4 was observed [δ 2.62, d, J(HH) 15 Hz], the other half of the signal being obscured by that of the PEt_3 groups. Nevertheless, the assignment was confirmed by using $[PtD(Me_2CO)(PEt_3)_2][BF_4]$ as a precursor to yield (**3a**) with a deuterium labelled BC(H)(D)C_6H_4Me-4 group. Measurement of the ^{2}H-{^{1}H} n.m.r. spectrum of this species revealed two resonances at δ 2.0 and 2.6 of equal intensity corresponding to the presence of the two diastereoisomeric forms. In the ^{11}B-{^{1}H} n.m.r. spectrum, the signal at δ 36.2 p.p.m. [J(PtB) *ca.* 400 Hz] may be ascribed to the BPt group, and that at 10.6 p.p.m. to the $BCH_2C_6H_4$Me-4 fragment. Neither of these signals showed ^{1}H–^{11}B coupling in a ^{11}B n.m.r. spectrum.

The ^{31}P-{^{1}H} n.m.r. spectrum of (**3a**) had the expected three resonances, and that at δ −18.3 p.p.m. may be assigned to the W(PMe_3) group because of the observation of ^{183}W–^{31}P coupling (204 Hz). Of the remaining two signals (Table 3), that at δ 13.7 p.p.m. is extremely broad due to ^{11}B–^{31}P coupling, and is therefore assigned to the PEt_3 group *trans* to B(3) of Figure 2, *i.e.* P(1).

The spectroscopic properties of compounds (**3b**)—(**3d**) were similar to those of (**3a**), with some differences arising through variations in the donor ligand added to the tungsten centre. Thus the i.r. spectrum of (**3b**) (Table 1) shows three CO stretching bands, and the ^{13}C-{^{1}H} n.m.r. spectrum (Table 2) has three carbonyl resonances. The i.r. spectrum of (**3c**) showed a characteristic absorption for the CNBu^t ligand at 2 131 cm^{-1}, and corresponding signals for this group are observed in the ^{1}H and ^{13}C-{^{1}H} n.m.r. spectra. The P*H*Ph_2 ligand in (**3d**) gives a characteristic doublet signal [J(PH) 396 Hz] in the ^{1}H n.m.r. spectrum at δ 5.29. Most significantly the n.m.r. spectra of (**3b**)—(**3d**) show diagnostic signals for the presence of a μ-H ligand, and a B–Pt σ bond. In the ^{1}H n.m.r. spectra the bridging–hydrido ligand resonances are at δ −8.81 (**3b**), −8.72 (**3c**), and −8.29 (**3d**), while in the ^{11}B-{^{1}H} n.m.r. spectra the Pt–B peaks are at δ 44.0 (**3b**), 41.2 (**3c**), and 36.6 p.p.m. (**3d**).

As noted above, the reactivity of (**2a**) towards electron pair donor molecules is as expected, in view of the electron deficient nature of the WC_2B_9 cage in the precursor. Regeneration of a *closo* cage in the products (**3a**)—(**3d**) is consistent with an electron count of 16 and 18 at the platinum and tungsten centres, respectively, and 13 skeletal electron pairs in the

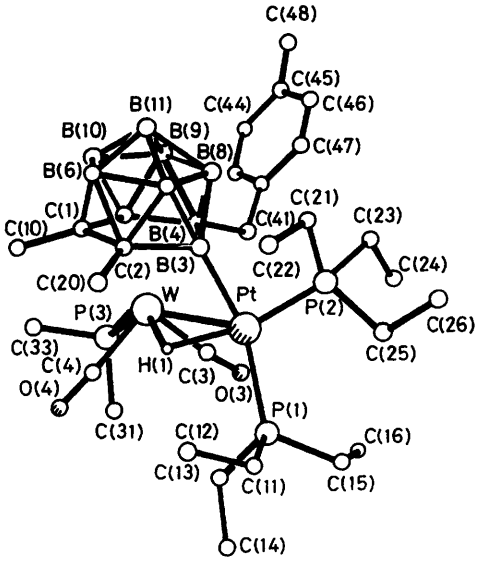

Figure 2. The molecular structure of $[PtW(\mu\text{-}H)\{\mu\text{-}\sigma\text{:}\eta^5\text{-}C_2B_9H_7(CH_2C_6H_4Me\text{-}4)Me_2\}(CO)_2(PMe_3)(PEt_3)_2]$ (**3a**) showing the atom-labelling scheme

WC_2B_9 cage. The formation of a bridging hydrido ligand and a B–Pt σ bond is somewhat unexpected, although the reaction between (**2b**) and CO described below sheds some light on the likely course of reaction.

As mentioned earlier, it was not possible to separate (**2b**) and (**2c**). Hence a reaction between a mixture of these species and CO was studied in the hope that the expected products $[PtW(\mu\text{-}H)\{\mu\text{-}\sigma\text{:}\eta^5\text{-}C_2B_9H_7(R)Me_2\}(CO)_3(PEt_3)_2]$ [(**3e**), R = H; (**3f**), R = Et] might be separable. In practice a more complex mixture was produced, ^1H n.m.r. studies indicating the presence of at least three components, two containing Pt(μ-H)W groups, and one containing a B–H → Pt group. Complete separation by column chromatography or fractional crystallisation proved impossible, not least because two of the products existed in equilibrium in the solution. Crystals suitable for an *X*-ray diffraction study were obtained, although as described below, all three species were present in the crystals. Nevertheless, the structures were determined, and a full interpretation of the i.r. and n.m.r. data became possible.

The essential results of the *X*-ray study are summarised in Table 6. The asymmetric unit contained two crystallographically and chemically distinct molecules designated I and II. A further complication arose in that molecule I exhibited a partial occupancy at one crystallographic site due to the presence of both (**3e**) and (**3f**) in a 1:4 ratio. Figure 3 depicts the molecular structure of (**3f**), but in the crystal disorder occurs at the *exo*-polyhedral substituent site at B(14) which may be an Et group (**3f**, 80%) or an H atom (**3e**, 20%). This results from an unusually complicated co-crystallisation which is understandable in terms of the reaction chemistry.

Compound (**3f**) is structurally and chemically analogous to (**3a**) with a third CO group ligating the tungsten instead of a PMe_3 group and an Et substituent on the C_2B_9 framework instead of a $CH_2C_6H_4Me$-4 fragment. The Pt–W separation [2.902(1) Å] is very similar to that in (**3a**) [2.843(2) Å] and both distances are comparable with that found [2.895(1) Å] in the compound $[PtW(\mu\text{-}H)\{\mu\text{-}CH(C_6H_4Me\text{-}4)\}(CO)_2(PMe_3)_2(\eta\text{-}C_5H_5)]$ which also has a bridging hydride ligand.[9] Thus (**3f**) is the expected product from (**2c**) and CO, while the presence of (**3e**) corresponds to the molecular structure anticipated by addition of CO to (**2b**).

Molecule II (Figure 4) is chemically and crystallographically

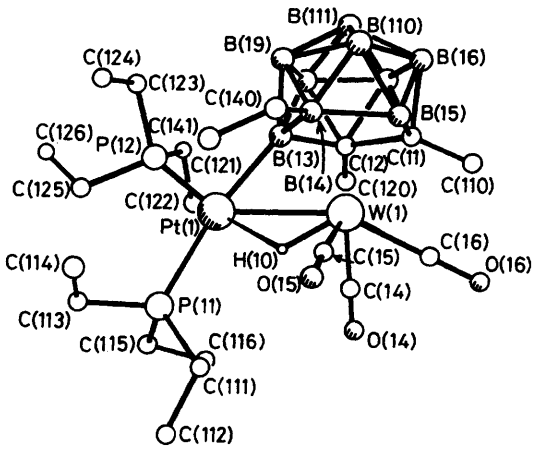

Figure 3. The molecular structure of $[PtW(\mu\text{-}H)\{\mu\text{-}\sigma\text{:}\eta^5\text{-}C_2B_9H_7(Et)Me_2\}(CO)_3(PEt_3)_2]$ (**3f**). The molecular structure of (**3e**) is identical apart from substitution of the ethyl group C(140)C(141) in the former by H in the latter

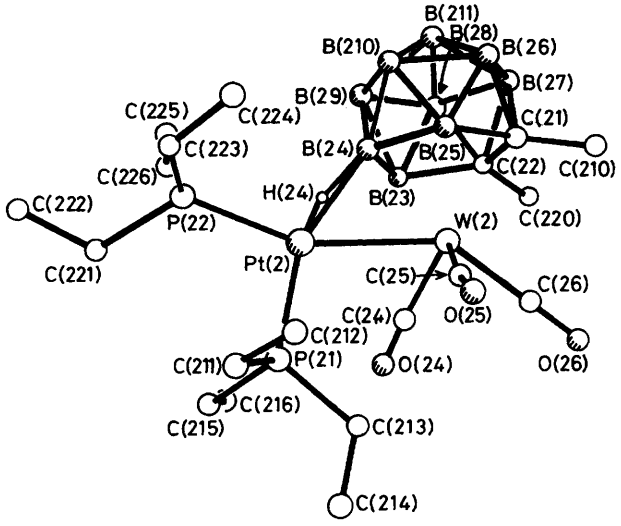

Figure 4. The molecular structure of $[PtW(CO)_3(PEt_3)_2(\eta^5\text{-}C_2B_9H_9Me_2)]$ (**4**) showing the atom-labelling scheme

distinct from I, and is in fact $[PtW(CO)_3(PEt_3)_2(\eta^5\text{-}C_2B_9H_9Me_2)]$ (**4**), an isomer of (**3e**). Compound (**4**) has a Pt–W bond [2.818(1) Å] bridged by a three-centre two-electron B–H → Pt bond. Similar bonds in heteronuclear and homonuclear dimetal compounds have been observed previously in Mo,[2c] W,[2c] Ru,[2b] and Rh[23] systems. The Pt(2)–B(24) separation [2.41(2) Å] is significantly longer than the Pt(1)–B(13) distance [2.15(2) Å] in molecule I, and the bridging hydrogen atom H(24) was located and refined. The C_2B_9W cage exhibits *closo* geometry, with W(2) removed from a position above the centroid of the B(26)B(27)B(28)B(29)B(210) ring towards B(24) by 0.18 Å. This 'slippage' is similar to that observed previously in related bridge systems.[2b,c] The Pt(2)–W(2) vector lies essentially parallel to the above five boron atoms.

As discussed below, spectroscopic data reveal an equilibrium in solution between the isomers (**4**) and (**3e**). This requires breaking the BH → Pt bond and formation of a B–Pt bond. Moreover, generation of the latter requires rotation of the *nido* face of the C_2B_9 cage and migration of a BH hydrogen atom to the metal–metal bond since in (**3e**) the boron σ bonded to platinum is B(13) and not B(14) (Figure 3). Due to its 20% site

Table 7. Crystal data and experimental parameters[a]

Compound	(2a)	(3a)	(3e), (3f), and (4)
Formula	$C_{26}H_{53}B_9O_2P_2PtW{\cdot}CH_2Cl_2$	$C_{29}H_{62}B_9O_2P_3PtW$	$C_{19}H_{45}B_9O_3P_2PtW$ (60%) $C_{21}H_{49}B_9O_3P_2PtW$ (40%)
M	1 020.8	1 012.0	859.7 (60%), 887.7 (40%) 870.9 (mean)
Crystal system	Monoclinic	Triclinic	Monoclinic
Crystal habit	Irregular	Hexagonal prism	Triangular prism
Colour	Orange	Orange	Orange
Space group	$P2_1/c$	$P\bar{1}$	$P2_1/n$
a/Å	11.893(2)	11.376(7)	17.390(3)
b/Å	15.233(3)	16.380(7)	17.731(6)
c/Å	22.153(3)	11.000(6)	21.220(4)
α/°		100.44(4)	
β/°	93.35(1)	85.92(5)	100.68(1)
γ/°		93.15(4)	
U/Å^3	4 007(1)	2 009(2)	6 430(3)
Z	4	2	8
D_c/g cm^{-3}	1.69	1.67	1.80
$F(000)$	1 975	988	3 330.2
μ(Mo-K_α)/cm^{-1}	66.9	65.8	81.6
Crystal size (mm)	0.25 × 0.20 × 0.20	0.4 × 0.4 × 0.5	0.5 × 0.4 × 0.2
Data unique	6 569	7 109	9 412
Data used[b]	3 679	5 743	6 112
Weighting scheme: g $w^{-1} = [\sigma^2(F) + g\lvert F\rvert^2]$	0.0009	0.0004	0.0005
$R(R')$	0.053 (0.054)	0.025 (0.027)	0.044 (0.042)
Largest final electron-density difference features (e Å^{-3})	+1.9, −1.3	+0.8, −0.9	+1.4, −1.1

[a] Nicolet $P3m$ automated diffractometer, operating at 298 K in a θ–2θ scan mode, $3 \leqslant \theta \leqslant 50°$, with Mo-$K_\alpha$ X-radiation (graphite monochromator), $\lambda = 0.710\,69$ Å. Crystals were grown from CH_2Cl_2–Et_2O and mounted in thin-walled glass capillaries under nitrogen. [b] Only data meeting the criterion $I \geqslant 3\sigma(I)$ were used in solution and refinement of the structures, after correction for Lorentz, polarization and X-ray absorption effects had been applied; the latter by an empirical method based on azimuthal scan data (ref. 28).

Table 8. Atomic positional parameters (fractional co-ordinates, × 10^4) with estimated standard deviations in parentheses for (2a)

Atom	x	y	z	Atom	x	y	z
Pt	3 322(1)	2 470(1)	2 404(1)	C(43)	−1 555(14)	4 066(13)	4 169(10)
W	1 813(1)	1 900(1)	3 113(1)	C(44)	−2 288(16)	4 325(14)	4 564(11)
P(1)	5 194(4)	2 716(4)	2 689(2)	C(45)	−2 013(16)	4 336(13)	5 176(10)
P(2)	3 064(4)	2 886(4)	1 407(2)	C(46)	−968(17)	4 118(13)	5 375(9)
C(3)	2 148(11)	3 200(12)	2 933(6)	C(47)	−184(15)	3 854(11)	4 958(8)
O(3)	2 209(11)	3 980(7)	2 913(6)	C(48)	−2 852(25)	4 635(19)	5 659(15)
C(4)	2 827(15)	1 135(12)	2 588(8)	C(11)	6 046(13)	3 387(11)	2 214(8)
O(4)	3 231(11)	582(9)	2 342(7)	C(12)	7 313(14)	3 456(13)	2 419(9)
C(1)	468(13)	1 154(12)	2 844(7)	C(13)	6 000(20)	1 722(16)	2 854(11)
C(10)	259(16)	738(15)	2 217(9)	C(14)	6 147(21)	1 238(17)	2 279(12)
C(2)	2 169(12)	1 075(12)	3 823(8)	C(15)	5 366(27)	3 119(22)	3 483(15)
C(20)	3 295(15)	608(15)	3 933(10)	C(16)	5 032(31)	3 872(25)	3 453(18)
B(3)	1 743(16)	2 017(13)	4 159(8)	C(21)	1 763(27)	2 733(23)	1 106(18)
B(4)	533(15)	2 523(14)	3 795(8)	C(22)	721(22)	3 070(18)	1 394(13)
B(5)	−141(12)	2 060(14)	3 089(9)	C(23)	3 690(40)	3 877(32)	993(22)
B(6)	972(19)	508(13)	3 495(10)	C(24)	3 545(31)	4 413(23)	1 394(19)
B(7)	1 258(18)	876(13)	4 332(10)	C(25)	3 974(38)	2 440(29)	814(23)
B(8)	315(18)	1 756(16)	4 431(11)	C(26)	3 923(23)	1 516(20)	785(14)
B(9)	−697(15)	1 804(13)	3 801(8)	C(S)	2 451(18)	8 175(22)	4 876(11)
B(10)	−548(18)	933(16)	3 277(11)	H(Sa)	2 213	7 648	5 069
B(11)	−186(17)	776(15)	4 042(9)	H(Sb)	1 942	8 644	4 958
C(41)	389(15)	3 547(11)	3 903(8)	Cl(S1)	2 439(6)	7 997(6)	4 118(3)
C(42)	−476(14)	3 826(11)	4 342(8)	Cl(S2)	3 769(8)	8 431(9)	5 167(4)

occupancy in molecule I, compound (**3e**) makes a relatively small contribution to the observed structure factors and therefore platinum bonding to B(14) cannot be entirely ruled out. Nevertheless, the ^{13}C-$\{^1H\}$ n.m.r. data, referred to below, strongly support a structure for (**3e**) exactly analogous to (**3a**) and (**3f**).

Examination of peak intensities in the n.m.r. spectra of solutions of the mixture of (**3e**), (**3f**), and (**4**) revealed that these species were formed in a ratio of *ca.* 1:4:1. Chromatography on alumina afforded two overlapping bands which were orange and pink, respectively. The pink eluate became orange on standing. Initially the i.r. spectra of the orange and pink fractions in CH_2Cl_2 solution showed six CO stretching bands at the same frequencies [2 013, 1 950, 1 940(sh), 1 902, 1 860(sh), and 1 850 cm^{-1}] but with different relative intensities. However, on standing the relative peak intensities in each fraction

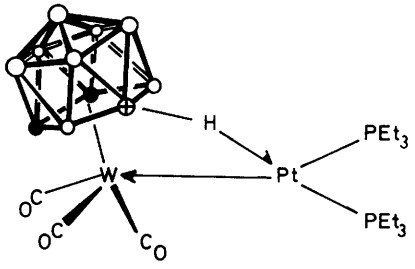

(4)

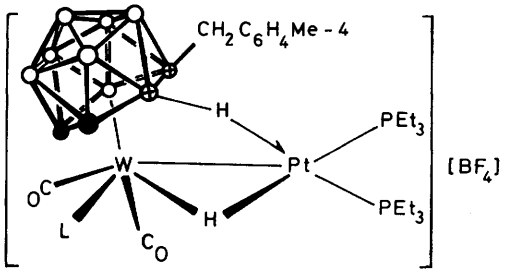

L

(5a) PMe_3

(5b) CO

(5c) $CNBu^t$

O BH ● CMe ⊕ B

changed, and in *ca.* 15 min the spectra of the two fractions became nearly identical.

Each of the species (**3a**), (**3f**), and (**4**) might be expected to show three i.r.-active CO stretching bands but the close similarity of the structures of (**3e**) and (**3f**) could well result in the absorptions for these species overlapping. That this occurs was shown by allowing a mixture to reach equilibrium in CH_2Cl_2, removing solvent *in vacuo*, dissolving the residue in Et_2O, and measuring the spectra in Et_2O. The bands observed (2 011, 1 955, 1 942, 1 900, 1 873, and 1 858 cm^{-1}) were shifted, due to change in solvent, but that at 1 900 cm^{-1} was asymmetric to high frequency. By applying the Fourier self-deconvolution resolution enhancement technique[24] this peak was resolved into two bands at 1 907 and 1 900 cm^{-1}. By comparison with the i.r. spectra of (**3b**) the bands at 2 011, 1 942, 1 907 and 1 900 cm^{-1} are assigned to (**3e**) and (**3f**); overlap occurring for the two higher frequency absorptions. The remaining bands at 1 955, 1 873, and 1 858 cm^{-1} can then be attributed to compound (**4**).

The i.r. spectra of the partially separated fractions indicated that the pink eluate was primarily compound (**4**), which on standing gave an equilibrium mixture (1:1) with (**3e**). The orange band consisted mainly of (**3e**) and (**3f**), but on standing the presence of (**4**) could be detected. The relatively short time required for these pink and orange eluates to reach equilibrium made it virtually impossible to obtain n.m.r. data for the initially separated fractions. However, assignment of important signals (Tables 2 and 3) for the individual species was possible based on relative peak intensities in the spectra of the fractions at equilibrium, and the assignments made for (**3b**).

The high-field region of the ^1H n.m.r. spectrum was especially informative. Sharp signals at δ −9.12 and −8.94 could be assigned to the Pt(μ-H)W groups in (**3e**) and (**3f**), respectively. Each shows coupling to two non-equivalent ^{31}P nuclei, with ^{195}Pt and ^{183}W satellite peaks. The broad signal at δ −7.06 is characteristic for a B–H → Pt group, and is accordingly assigned to compound (**4**). As expected, the ^1H spectrum of the pink eluate, mentioned above, after equilibrium has been attained, showed the peak at δ −8.94 at much reduced intensity, compared with the signal at δ −9.12 since only a small amount of (**3f**) was present.

As expected, the ^{13}C-{^1H} n.m.r. spectrum of the equilibrium mixture showed eight rather than nine CO resonances (Table 2), since the two carbonyl ligands *cis* to the platinum atom in compound (**4**) (Figure 4) are equivalent. Assignments made in Table 2 were facilitated by measuring fully coupled ^{13}C spectra which resulted in some CO resonances [(**3e**) and (**3f**)] showing coupling with the μ-H ligands, and by noting relative intensities, and the appearance of ^{183}W and ^{195}Pt satellite peaks.

The signal at δ 36.8 p.p.m. [J(PtC) 34 Hz] is characteristic for a C*Me* group in the C_2B_9 cage, and is assigned to (**3e**), while the resonance at δ 36.9 p.p.m. [J(PtC) 34 Hz] is assigned to (**3f**). Based on analysis of the ^{13}C-{^1H} n.m.r. spectrum of (**3a**), for which the structure was established by *X*-ray crystallography, the appearance of ^{195}Pt–^{13}C coupling on the resonance at δ 36.8 p.p.m. supports the supposition that in (**3e**) the platinum atom is σ bonded to a boron adjacent to a CMe group, *i.e.* B(13) of Figure 3. If the platinum were attached to B(14) the 34 Hz coupling would correspond to a ^4J(PtC) value which would be a most unlikely result.

The ^{11}B-{^1H} spectrum of the mixture of (**3e**), (**3f**), and (**4**) showed low-field signals with ^{195}Pt-^{11}B coupling (*ca.* 500 Hz) at δ 42.7 and 44.6 p.p.m., and these may be assigned to the B–Pt groups of (**3e**) and (**3f**), respectively, by analogy with the spectra of (**3a**)—(**3d**). A resonance at δ 21.4 p.p.m. [J(PtB) *ca.* 180 Hz] is assigned to the B–H → Pt group in (**4**), while a signal at δ 14.7 p.p.m. is attributed to the BEt group of (**3f**), since in a fully coupled ^{11}B spectrum it showed no ^1H–^{11}B coupling.

The observations of the equilibrium (**3e**) ⇌ (**4**) suggests that the transformations (**2a**) ⟶ (**3a**)—(**3d**), (**2b**) ⟶ (**3e**), and (**2c**) ⟶ (**3f**) may occur *via* intermediates with B–H → Pt bridge systems. For the reactions involving (**2a**) and (**2c**), because of the presence of the BR (R = $CH_2C_6H_4Me$-4 or Et) groups, the transformations must involve a boron atom in the C_2B_3 *nido* face of the cage which is adjacent to a CMe group. These intermediates, if involved, are evidently unstable with respect to the formation of (**3a**)—(**3d**) or (**3f**). However, for the reaction between (**2b**) and CO the absence of an alkyl substituent at B(24) (Figure 4) allows, perhaps for steric reasons, formation of a B–H → Pt bond at this site. Moreover, the resulting species (**4**) is essentially as stable as (**3e**) since the two exist in equilibrium.

Treatment of the compounds (**3a**)—(**3c**) with HBF_4·Et_2O in CH_2Cl_2 afforded the salts [$PtW(\mu\text{-}H)(CO)_2(L)(PEt_3)_2\{\eta^5\text{-}C_2B_9H_8(CH_2C_6H_4Me\text{-}4)Me_2\}$][$BF_4$] [(**5a**), L = PMe_3; (**5b**), L = CO; (**5c**), L = $CNBu^t$], characterised by the data given in Tables 1—3. The ^1H n.m.r. spectra of these complexes contained high-field signals due to the Pt(μ-H)W groups, but in addition

Table 9. Atomic positional parameters (fractional co-ordinates, × 10^4) with estimated standard deviations in parentheses for (**3a**)

Atom	*x*	*y*	*z*	Atom	*x*	*y*	*z*
Pt	328(1)	2 371(1)	2 502(1)	C(41)	3 291(5)	3 754(3)	3 203(5)
W	2 297(1)	1 785(1)	3 491(1)	C(42)	4 277(5)	4 339(3)	2 886(5)
P(1)	−1 404(1)	2 260(1)	3 801(1)	C(43)	5 312(5)	4 432(3)	3 494(5)
P(2)	−243(1)	3 050(1)	1 050(1)	C(44)	6 269(5)	4 904(3)	3 158(5)
P(3)	3 350(1)	1 831(1)	5 402(1)	C(45)	6 240(5)	5 338(3)	2 192(5)
C(3)	1 606(4)	2 700(3)	4 707(5)	C(46)	5 193(7)	5 293(4)	1 626(5)
O(3)	1 277(3)	3 274(2)	5 390(4)	C(47)	4 237(6)	4 804(4)	1 959(6)
C(4)	1 621(5)	796(4)	4 128(5)	C(48)	7 298(6)	5 835(4)	1 787(6)
O(4)	1 254(4)	195(3)	4 428(5)	C(11)	−2 455(5)	1 471(4)	3 077(6)
C(1)	3 683(4)	1 042(3)	1 968(5)	C(12)	−1 945(7)	650(5)	2 619(8)
C(10)	3 976(5)	216(3)	2 311(6)	C(13)	−1 156(5)	1 899(4)	5 241(5)
C(2)	2 433(4)	1 142(3)	1 403(5)	C(14)	−2 249(6)	1 755(5)	6 100(6)
C(20)	1 539(5)	416(4)	1 189(5)	C(15)	−2 318(5)	3 147(4)	4 359(6)
B(3)	2 068(5)	2 221(4)	1 682(5)	C(16)	−1 717(7)	3 859(5)	5 162(8)
B(4)	3 332(4)	2 813(4)	2 437(5)	C(21)	107(5)	2 582(4)	−549(5)
B(5)	4 267(5)	2 012(4)	2 634(5)	C(22)	−465(6)	1 706(4)	−899(6)
B(6)	3 652(6)	960(4)	377(6)	C(23)	469(5)	4 082(4)	1 110(6)
B(7)	2 623(5)	1 678(4)	207(5)	C(24)	233(7)	4 661(5)	2 351(8)
B(8)	3 182(5)	2 682(4)	786(5)	C(25)	−1 817(5)	3 232(4)	1 061(6)
B(9)	4 588(5)	2 560(4)	1 389(6)	C(26)	−2 234(6)	3 598(5)	−15(7)
B(10)	4 812(5)	1 488(4)	1 155(6)	C(31)	2 375(5)	1 788(4)	6 780(5)
B(11)	4 143(5)	1 902(4)	10(6)	C(32)	4 306(5)	2 743(4)	5 898(5)
				C(33)	4 315(5)	986(4)	5 487(6)

diagnostic resonances for the B–H → Pt bridge system were observed as broad signals at *ca.* δ −5.5 with ^{195}Pt satellite peaks [*J*(PtH) *ca.* 450 Hz]. In the ^{11}B-{^{1}H} spectra (Table 3) the low-field signals observed with (**3a**)—(**3c**), due to their B–Pt groups, are replaced in the spectra of (**5**) by signals at δ 9—12 p.p.m. attributed to the B–H → Pt fragments. For (**5c**) the peaks for the *B*$CH_2C_6H_4$Me-4 and *B*–H → Pt groups overlap.

It is significant that in the ^{13}C-{^{1}H} n.m.r. spectrum of (**5a**) coupling between the platinum and the cage CMe signals is less than the ^{195}Pt–^{13}C couplings to the CMe groups in (**3a**) (Table 2). This is clearly an effect resulting from the insertion of a hydrogen atom into the B–Pt σ bond.

The work described in this paper has demonstrated the unprecedented conversion of alkylidyne ligands terminally bound to tungsten into BCH_2R (R = C_6H_4Me-4 or Me) groups, which form part of C_2B_9 cage systems. Also unprecedented has been the observation for these 12-vertex carbametallaborane systems of *closo* to *iso-closo* (*hyper-closo*) to *closo* reaction sequences. The existence of a facile equilibrium between species with *exo*-polyhedral B–H → Pt and B–Pt bonds is also of considerable interest, and it is evident that further studies in this area[2,25] would add new dimensions to our knowledge of reactivity at dimetal centres.

Experimental

The experimental techniques used and the instrumentation employed has been described in previous Parts of this series.[2] Light petroleum refers to that fraction of b.p. 40—60 °C. The compounds [N(PPh$_3$)$_2$][W(≡CR)(CO)$_2$(η^5-$C_2B_9H_9Me_2$)] (R = C_6H_4Me-4 or Me)[2a] and [PtH(Me$_2$CO)(PEt$_3$)$_2$][BF$_4$][26] were prepared by methods described earlier. Analytical and other data for the new compounds are given in Table 1.

Synthesis of [PtW(CO)$_2$(PEt$_3$)$_2${η^6-$C_2B_9H_8$($CH_2C_6H_4$Me-4)Me$_2$}].—The compound *trans*-[PtH(Cl)(PEt$_3$)$_2$] (0.50 g, 1.06 mmol) in acetone (5 cm^3) was treated with $AgBF_4$ (0.21 g, 1.06 mmol) to generate [PtH(Me$_2$CO)(PEt$_3$)$_2$][BF$_4$] *in situ*. After removing AgCl by filtration, and washing the AgCl with acetone (5 cm^3), the combined filtrates were slowly added to a stirred acetone (20 cm^3) solution of (**1a**) (1.11 g, 1.06 mmol) at −30 °C. There was an immediate colour change from orange to orange-brown. The mixture was stirred (0.5 h), and then solvent was removed slowly (*ca.* 2 h) *in vacuo* at −30 °C. The residue was extracted with cold (*ca.* −30 °C) Et_2O–CH_2Cl_2 (30 cm^3, 3:2), and the extracts chromatographed on an alumina column (2 × 15 cm) maintained at −30 °C. Elution with the same solvent mixture afforded an orange eluate, which was concentrated *in vacuo* to *ca.* 10 cm^3 and cooled to *ca.* −78 °C, to give orange-red *crystals* of [PtW(CO)$_2$(PEt$_3$)$_2${η^6-$C_2B_9H_8$-($CH_2C_6H_4$Me-4)Me$_2$}] (**2a**) (0.81 g).

Reaction between [PtH(Me$_2$CO)(PEt$_3$)$_2$][BF$_4$] *and* [N(PPh$_3$)$_2$][W(≡CMe)(CO)$_2$(η^5-$C_2B_9H_9Me_2$)].—An acetone (20 cm^3) solution of [PtH(Me$_2$CO)(PEt$_3$)$_2$][BF$_4$] (1.03 mmol), prepared as described above, was added slowly to a stirred suspension of (**1b**) (1.00 g, 1.03 mmol) in acetone (10 cm^3) at −40 °C. There was a rapid colour change from yellow to orange, and all of (**1b**) present appeared to dissolve. The mixture was stirred for a further 2 h, and then solvent was removed *in vacuo* at −30 °C, a process taking a further 2 h. The residue was extracted with Et_2O–CH_2Cl_2 (30 cm^3, 2:1) at −30 °C, and the extracts chromatographed on an alumina column (*ca.* 2 × 30 cm) at −40 °C, eluting with the same solvent mixture. A broad yellow-brown eluate was collected. Solvent was removed *in vacuo* and the residue recrystallised from the same solvent mixture (*ca.* 15 cm^3) at −78 °C giving orange *crystals* (0.31 g) of a *ca.* 1:2 mixture of [PtW(CO)$_2$(PEt$_3$)$_2$(η^6-$C_2B_9H_9Me_2$)] (**2b**) and [PtW(CO)$_2$(PEt$_3$)$_2${η^6-$C_2B_9H_8$(Et)Me$_2$}] (**2c**).

Reactions of [PtW(CO)$_2$(PEt$_3$)$_2${η^6-$C_2B_9H_8$($CH_2C_6H_4$Me-4)Me$_2$}] *with Donor Molecules*.—(*i*) A CH_2Cl_2 (10 cm^3) solution of (**2a**) (0.22 g, 0.24 mmol) at −30 °C was treated with PMe_3 (50 μl, 0.50 mmol). The mixture was warmed to room temperature, and solvent was removed *in vacuo*. The residue was then redissolved in CH_2Cl_2 (1 cm^3). Addition of Et_2O (5 cm^3) afforded orange *microcrystals* of [PtW(μ-H){μ-σ:η^5-$C_2B_9H_7$-($CH_2C_6H_4$Me-4)Me$_2$}(CO)$_2$(PMe$_3$)(PEt$_3$)$_2$] (**3a**) (0.19 g).

(*ii*) A CH_2Cl_2 (10 cm^3) solution of (**2a**) (0.31 g, 0.34 mmol) at −30 °C was stirred under an atmosphere of CO for 5 min. The solution was warmed to room temperature, and solvent was removed *in vacuo*. The residue was redissolved in CH_2Cl_2 (1

Table 10. Atomic positional parameters (fractional co-ordinates, × 10^4) with estimated standard deviations in parentheses for (**3e**), (**3f**), and (**4**)

Atom	*x*	*y*	*z*	Atom	*x*	*y*	*z*
Pt(1)	3 921(1)	1 508(1)	1 557(1)	Pt(2)	9 014(1)	1 337(1)	1 951(1)
W(1)	2 899(1)	2 155(1)	453(1)	W(2)	8 595(1)	2 154(1)	799(1)
C(14)	2 232(9)	1 272(10)	560(6)	C(24)	7 957(10)	1 238(10)	640(7)
O(14)	1 826(7)	744(7)	605(5)	O(24)	7 552(7)	712(7)	521(6)
C(15)	3 513(12)	1 779(10)	−147(7)	C(25)	9 645(9)	1 792(8)	776(6)
O(15)	3 873(9)	1 575(9)	−531(6)	O(25)	10 312(6)	1 659(6)	766(5)
C(16)	2 151(9)	2 113(8)	−374(6)	C(26)	8 555(11)	2 027(10)	−115(7)
O(16)	1 742(7)	2 102(7)	−863(4)	O(26)	8 496(9)	1 929(8)	−667(5)
P(11)	4 249(2)	223(2)	1 452(2)	P(21)	9 385(2)	173(2)	1 678(2)
C(111)	3 918(10)	−129(8)	628(6)	C(211)	10 362(8)	−73(9)	2 088(6)
C(112)	4 087(12)	−972(9)	525(7)	C(212)	10 971(8)	460(11)	1 926(8)
C(113)	5 314(9)	22(9)	1 586(7)	C(213)	9 402(8)	−29(8)	827(6)
C(114)	5 770(12)	537(13)	1 234(10)	C(214)	9 784(11)	−772(9)	696(7)
C(115)	3 841(9)	−466(9)	1 940(7)	C(215)	8 763(8)	−588(8)	1 888(6)
C(116)	2 946(10)	−476(12)	1 782(9)	C(216)	7 884(10)	−486(10)	1 646(9)
P(12)	4 434(3)	1 737(2)	2 598(2)	P(22)	9 252(3)	1 152(2)	3 048(2)
C(121)	3 711(10)	1 839(9)	3 122(6)	C(221)	9 231(8)	241(8)	3 430(6)
C(122)	3 191(14)	1 179(12)	3 161(8)	C(222)	9 309(11)	216(11)	4 164(6)
C(123)	5 051(10)	2 546(8)	2 757(8)	C(223)	10 246(11)	1 467(11)	3 433(8)
C(124)	5 748(10)	2 519(14)	2 378(12)	C(224)	10 518(15)	2 164(11)	3 231(10)
C(125)	5 066(10)	1 012(9)	3 018(7)	C(225)	8 579(9)	1 702(9)	3 410(6)
C(126)	5 383(15)	1 178(11)	3 745(7)	C(226)	7 731(10)	1 459(11)	3 188(9)
C(11)	2 215(8)	3 259(7)	672(5)	C(21)	8 658(12)	3 494(9)	762(8)
C(12)	2 572(7)	2 817(7)	1 353(5)	C(22)	7 732(10)	3 210(10)	704(7)
B(13)	3 581(9)	2 667(10)	1 393(7)	B(25)	9 213(12)	3 131(10)	1 446(9)
B(14)	3 858(9)	3 131(11)	683(7)	B(24)	8 546(11)	2 617(10)	1 812(7)
B(15)	2 957(12)	3 469(10)	226(7)	B(23)	7 620(11)	2 621(11)	1 299(9)
B(16)	2 581(11)	4 166(10)	684(8)	B(26)	8 876(16)	4 073(11)	1 392(11)
B(17)	2 351(11)	3 781(9)	1 381(7)	B(27)	7 968(15)	4 135(13)	945(9)
B(18)	3 236(11)	3 381(9)	1 829(7)	B(28)	7 327(15)	3 601(14)	1 299(10)
B(19)	4 000(10)	3 555(9)	1 433(7)	B(29)	7 868(15)	3 195(12)	2 019(10)
B(110)	3 565(11)	4 081(10)	720(7)	B(210)	8 856(17)	3 501(11)	2 094(11)
B(111)	3 243(11)	4 227(11)	1 434(8)	B(211)	8 084(18)	4 130(12)	1 769(11)
C(110)	1 356(8)	3 232(10)	377(7)	C(220)	7 165(12)	3 223(12)	61(7)
C(120)	2 037(8)	2 355(9)	1 668(6)	C(210)	8 967(13)	3 762(10)	185(8)
C(140)	4 643(17)	3 055(18)	329(13)				
C(141)	5 146(24)	2 471(25)	573(17)				

cm^3), and Et_2O (3 cm^3) added to give orange *microcrystals* of $[PtW(\mu\text{-}H)\{\mu\text{-}\sigma\text{:}\eta^5\text{-}C_2B_9H_7(CH_2C_6H_4Me\text{-}4)Me_2\}(CO)_3(PEt_3)_2]$ (**3b**) (0.28 g).

(*iii*) Similarly, (**2a**) (0.19 g, 0.20 mmol) in CH_2Cl_2 (5 cm^3) at −30 °C was treated with $CNBu^t$ (0.19 mmol). After warming to room temperature, solvent was removed *in vacuo*, and the residue dissolved in Et_2O–CH_2Cl_2 (10 cm^3, 3:2) and chromatographed on an alumina column (3 × 20 cm). Elution with the same solvent mixture gave an orange eluate. The latter was concentrated to *ca.* 1 cm^3, and treated with Et_2O (*ca.* 3 cm^3) to give orange *microcrystals* of $[PtW(\mu\text{-}H)\{\mu\text{-}\sigma\text{:}\eta^5\text{-}C_2B_9H_7(CH_2C_6H_4Me\text{-}4)Me_2\}(CO)_2(CNBu^t)(PEt_3)_2]$ (**3c**) (0.10 g).

(*iv*) A CH_2Cl_2 (10 cm^3) solution of (**2a**) (0.15 g, 0.16 mmol) at −30 °C was treated with $PHPh_2$ (0.16 mmol). After warming to room temperature solvent was removed *in vacuo*. The residue was dissolved in Et_2O–CH_2Cl_2 (10 cm^3, 4:1) and chromatographed. Elution with the same solvent mixture gave a yellow-orange eluate. After concentration to *ca.* 1 cm^3, addition of Et_2O (*ca.* 3 cm^3) gave pale orange *microcrystals* of $[PtW(\mu\text{-}H)\{\mu\text{-}\sigma\text{:}\eta^5\text{-}C_2B_9H_7(CH_2C_6H_4Me\text{-}4)Me_2\}(CO)_2(PHPh_2)(PEt_3)_2]$ (**3d**) (0.12 g).

Reaction between Carbon Monoxide and a Mixture of the Compounds $[PtW(CO)_2(PEt_3)_2\{\eta^6\text{-}C_2B_9H_8(R)Me_2\}]$ (R = H *or* Et).—A CH_2Cl_2 (5 cm^3) solution of a mixture of (**2b**) and (**2c**) (0.15 g, 1:2) at −30 °C was stirred under CO (1 atm) for *ca.* 5 min. After warming to room temperature, solvent was removed *in vacuo* affording an orange solid (0.15 g) which was identified spectroscopically as a mixture of $[PtW(\mu\text{-}H)\{\mu\text{-}\sigma\text{:}\eta^5\text{-}C_2B_9H_7(R)Me_2\}(CO)_3(PEt_3)_2]$ [(**3e**), R = H; (**3f**), R = Et] and $[PtW(CO)_3(PEt_3)_2(\eta^5\text{-}C_2B_9H_9Me_2)]$ (**4**). The solid was dissolved in Et_2O–CH_2Cl_2 (10 cm^3, 3:1) and chromatographed, eluting with the same solvent mixture. This produced overlapping orange and pink bands on the column. Spectroscopic analysis of the material obtained from the eluates revealed that the orange *microcrystals* were a mixture of (**3e**), (**3f**), and (**4**), and the pink microcrystals were a mixture of (**3e**) and (**4**).

Protonation of the Complexes $[PtW(\mu\text{-}H)\{\mu\text{-}\sigma\text{:}\eta^5\text{-}C_2B_9H_7(CH_2C_6H_4Me\text{-}4)Me_2\}(CO)_2(L)(PEt_3)_2]$ (L = PMe_3, CO, *or* $CNBu^t$).—(*i*) A CH_2Cl_2 (3 cm^3) solution of (**3a**) (0.16 g, 0.15 mmol) was treated with $HBF_4{\cdot}Et_2O$ (25 μl, 0.18 mmol). Solvent was removed *in vacuo*, and the residue was washed with Et_2O (2 × 2 cm^3). Crystallisation from Et_2O–CH_2Cl_2 (2 cm^3, 2:1) afforded orange *microcrystals* of $[PtW(\mu\text{-}H)(CO)_2(PMe_3)(PEt_3)_2\{\eta^5\text{-}C_2B_9H_8(CH_2C_6H_4Me\text{-}4)Me_2\}][BF_4]$ (**5a**) (0.14 g).

(*ii*) Similarly, (**3b**) (0.11 g, 0.11 mmol) in CH_2Cl_2 (3 cm^3) with $HBF_4{\cdot}Et_2O$ (20 μl, 0.15 mmol) gave orange *microcrystals* of $[PtW(\mu\text{-}H)(CO)_3(PEt_3)_2\{\eta^5\text{-}C_2B_9H_8(CH_2C_6H_4Me\text{-}4)Me_2\}][BF_4]$ (**5b**).

(*iii*) The compound $[PtW(\mu\text{-}H)(CO)_2(CNBu^t)(PEt_3)_2\{\eta^5\text{-}C_2B_9H_8(CH_2C_6H_4Me\text{-}4)Me_2\}][BF_4]$ (**5c**) (0.11 g) was prepared in a similar manner from (**3c**) (0.12 g, 0.12 mmol) and $HBF_4{\cdot}Et_2O$ (17 μl, 0.12 mmol).

Crystal-structure Determinations.—The crystal and other experimental data are summarised in Table 7. The structures

were solved, and all non-hydrogen atoms located by conventional heavy-atom and difference Fourier methods, with refinement by blocked-cascade least squares. For (**2a**), all non-hydrogen atoms were refined with anisotropic thermal parameters; except for the carbon atoms of the PEt_3 ligands which were refined isotropically. Hydrogen atoms attached to carbon were included in calculated positions (C–H 0.96 Å) with chemically related hydrogen atoms being given common isotropic thermal parameters (1.2 times $U_{equiv.}$ of parent carbon atom). Hydrogen atoms attached to boron were not located, and were therefore not included in the calculations.

For (**3a**), all non-hydrogen atoms were refined anisotropically. Hydrogen atoms bonded to C(41), C(43), C(44), C(46), and C(47) or to boron were located and refined isotropically. All CH_3 and C_2H_5 hydrogen atoms were treated as for (**2a**). The μ-H(1) atom was located as the predominant peak in an electron-density difference map, after all other atoms had been included, and H(1) was refined isotropically.

For the crystal containing (**3e**), (**3f**), and (**4**), the asymmetric unit contains two crystallographically independent and chemically inequivalent molecules, designated I and II in the following discussion. A further complication arose because I exhibited a partial occupancy of one crystallographic site, that of the *exo*-polyhedral substituent on B(14) [H (20%) or Et (80%)], corresponding to the two alternative products (**3e**) and (**3f**), respectively. Moreover, I (**3e**) and II (**4**) are isomers. Thus an unusually complicated co-crystallisation had occurred among three structurally very similar compounds (see Results and Discussion section).

Patterson solution of the structure revealed the four independent heavy-atom sites. Some peaks found in subsequent Fourier difference density maps indicated that molecule I corresponded to the two products (**3e**) and (**3f**) co-crystallised in a 1:4 ratio. Following extensive exploration of possible models, the most tractable by refinement was one in which C(140) and C(141) in I were included with site occupancies of 0.8.

For I, all non-hydrogen atoms were refined anisotropically, except C(140) and C(141) which were isotropically refined. Hydrogens with unit site occupancy attached to carbon or boron were included in calculated positions (C–H 0.96 Å, B–H 1.1Å with U_{iso} equal to 1.2 times $U_{equiv.}$ of the attached carbon, or boron atom). For B–H, the hydrogen atoms were set collinear with their parent boron atoms and the centroid of the 10-atom C_2B_8 fragment formed by C(11), C(12), and B(13)—B(110).[27] The bridging ligand H(10) was located and refined isotropically. Hydrogen atoms with $< 100\%$ site occupancy were not included in the refinement.

For molecule II, all non-hydrogen atoms were refined anisotropically, and the hydrogen atoms were included in calculated positions and treated as for I, apart from H(24) which was located and refined isotropically.

All calculations were carried out on an Eclipse S230 (Data General) computer with the SHELXTL system of programs.[28] Atomic scattering factors and corrections for anomalous dispersion were taken from ref. 29. The atomic co-ordinates are listed in Tables 8—10.

Acknowledgements

We thank the S.E.R.C. for a research studentship (to C. M. N.) and the U.S. Air Force Office of Scientific Research (Grant 86–0125) for partial support.

References

1 F-E. Baumann, J. A. K. Howard, O. Johnson, and F. G. A. Stone, *J. Chem. Soc., Dalton Trans.*, in the press.
2 (*a*) M. Green, J. A. K. Howard, A. P. James, C. M. Nunn, and F. G. A. Stone, *J. Chem. Soc., Dalton Trans.*, 1987, 61; (*b*) M. Green, J. A. K. Howard, A. N. de M. Jelfs, O. Johnson, and F. G. A. Stone, *ibid.*, p. 73; (*c*) M. Green, J. A. K. Howard, A. P. James, A. N. de M. Jelfs, C. M. Nunn, and F. G. A. Stone, *ibid.*, p. 81.
3 R. Hoffmann, *Angew. Chem., Int. Ed. Engl.*, 1982, **21**, 711.
4 F. G. A. Stone, *Angew. Chem., Int. Ed. Engl.*, 1984, **23**, 89.
5 J. H. Davis and C. M. Lukehart, *Organometallics*, 1984, **3**, 1763.
6 M. Green, J. A. K. Howard, A. P. James, A. N. de M. Jelfs, C. M. Nunn, and F. G. A. Stone, *J. Chem. Soc., Chem. Commun.*, 1985, 1778.
7 M. J. Attfield, J. A. K. Howard, A. N. de M. Jelfs, C. M. Nunn, and F. G. A. Stone, *J. Chem. Soc., Chem. Commun.*, 1986, 918.
8 M. R. Awang, J. C. Jeffery, and F. G. A. Stone, *J. Chem. Soc., Dalton Trans.*, 1986, 165.
9 J. C. Jeffery, I. Moore, and F. G. A. Stone., *J. Chem. Soc., Dalton Trans.*, 1984, 1571 and refs. therein.
10 N. N. Greenwood, *Chem. Soc. Rev.*, 1984, **13**, 353; J. E. Crook, M. Elrington, N. N. Greenwood, J. D. Kennedy, and J. D. Woolins, *Polyhedron*, 1984, **3**, 901; J. E. Crook, M. Elrington, N. N. Greenwood, J. D. Kennedy, M. Thornton-Pett, and J. D. Woolins, *J. Chem. Soc., Dalton Trans.*, 1985, 2407.
11 J. D. Kennedy, *Inorg. Chem.*, 1986, **25**, 111.
12 C. W. Jung, R. T. Baker, C. B. Knobler, and M. F. Hawthorne, *J. Am. Chem. Soc.*, 1980, **102**, 5782; C. W. Jung, R. T. Baker, and M. F. Hawthorne, *J. Am. Chem. Soc.*, 1981, **103**, 810.
13 R. T. Baker, *Inorg. Chem.*, 1986, **25**, 109.
14 R. L. Johnston and D. M. P. Mingos, *Inorg. Chem.*, 1986, **25**, 3321.
15 M. J. Chetcuti, K. Marsden, I. Moore, F. G. A. Stone, and P. Woodward, *J. Chem. Soc., Dalton Trans.*, 1982, 1749.
16 J. C. Jeffery, J. C. V. Laurie, I. Moore, H. Razay, and F. G. A. Stone, *J. Chem. Soc., Dalton Trans.*, 1984, 1563.
17 G. A. Carriedo, G. P. Elliott, J. A. K. Howard, D. B. Lewis, and F. G. A. Stone, *J. Chem. Soc., Chem. Commun.*, 1984, 1585.
18 S. V. Hoskins, A. P. James, J. C. Jeffery, and F. G. A. Stone, *J. Chem. Soc., Dalton Trans.*, 1986, 1709.
19 R. G. Teller and R. Bau, *Struct. Bonding (Berlin)*, 1981, **44**, 59.
20 A. G. Orpen, *J. Chem. Soc., Dalton Trans.*, 1980, 2509.
21 J. C. Jeffery, C. Sambale, M. F. Schmidt, and F. G. A. Stone, *Organometallics*, 1982, **1**, 1597.
22 J. Browning, P. L. Goggin, R. J. Goodfellow, N. W. Hurst, L. G. Mallinson, and M. Murray, *J. Chem. Soc., Dalton Trans.*, 1978, 872.
23 R. T. Baker, R. E. King, C. Knobler, C. A. O'Con, and M. F. Hawthorne, *J. Am. Chem. Soc.*, 1978, **100**, 8266; P. E. Behnken, T. B. Marder, R. T. Baker, C. B. Knobler, M. R. Thompson, and M. F. Hawthorne, *ibid.*, 1985, **107**, 932.
24 J. K. Kauppiner, D. J. Moffatt, H. H. Mantsch, and D. G. Cameron, *Appl. Spectrosc.*, 1981, **35**, 27.
25 J. A. K. Howard, A. P. James, A. N. de M. Jelfs, C. M. Nunn, and F. G. A. Stone, *J. Chem. Soc., Dalton Trans.*, 1987, 1221.
26 D. Afzal, P. G. Lenhert, and C. M. Lukehart, *J. Am. Chem. Soc.*, 1984, **106**, 3050.
27 P. Sherwood, Program to generate BH atom co-ordinates in icosahedral borane fragments, Bristol University, 1986.
28 G. M. Sheldrick, SHELXTL programs for use with the Nicolet *X*-Ray System, Cambridge, 1976; updated Göttingen, 1981.
29 'International Tables for *X*-Ray Crystallography,' Kynoch Press, Birmingham, 1974, vol. 4.

Received 9*th December* 1986; *Paper* 6/2369